SKB

TECHNICAL REPORT 90-37

The influence of fracture mineral/groundwater interaction on the mobility of U, Th, REE and other trace elements

Ove Landström[1], Eva-Lena Tullborg[2]

[1] Studsvik AB, Nyköping
[2] SGAB, Gothenburg

December 1990

SVENSK KÄRNBRÄNSLEHANTERING AB
SWEDISH NUCLEAR FUEL AND WASTE MANAGEMENT CO

BOX 5864 S-102 48 STOCKHOLM

TEL 08-665 28 00 TELEX 13108 SKB S
TELEFAX 08-661 57 19

THE INFLUENCE OF FRACTURE MINERAL/GROUNDWATER INTERACTION ON THE MOBILITY OF U, Th, REE AND OTHER TRACE ELEMENTS

Ove Landström[1], Eva-Lena Tullborg[2]

1 Studsvik AB, Nyköping
2 SGAB, Gothenburg

December 1990

This report concerns a study which was conducted for SKB. The conclusions and viewpoints presented in the report are those of the author(s) and do not necessarily coincide with those of the client.

Information on SKB technical reports from 1977-1978 (TR 121), 1979 (TR 79-28), 1980 (TR 80-26), 1981 (TR 81-17), 1982 (TR 82-28), 1983 (TR 83-77), 1984 (TR 85-01), 1985 (TR 85-20), 1986 (TR 86-31), 1987 (TR 87-33), 1988 (TR 88-32) and 1989 (TR 89-40) is available through SKB.

SVERIGES GEOLOGISKA AB
Division: Ingenjörsgeologi
Beställare: SKB

Datum: 90-10-28
Id-nr: IRAP 90414

THE INFLUENCE OF FRACTURE MINERAL/GROUNDWATER INTERACTION ON THE MOBILITY OF U, Th, REE AND OTHER TRACE ELEMENTS

Ove Landström[1]
Eva-Lena Tullborg[2]

[1] Studsvik AB, 611 82 NYKÖPING
[2] SGAB, Pusterviksgatan 2, 413 01 GÖTEBORG

ABSTRACT

Trace element analyses including U, Th and REE have been carried out on groundwater samples, fracture coatings and rock samples from drill cores. The influence of fracture mineral/groundwater interaction on the mobility of these elements is discussed. Compared to the host rocks the levels and ranges of element contents in the fracture fillings are usually much higher, reflecting the wide range in sorption capacities of different fracture-filling minerals.

In order to use the elements analysed as chemical analogues to predictions of actinide migration, the following cases are discussed:

1) Redistribution of elements in connection to clay forming alteration processes and preferential sorption of elements on clay minerals.
2) Occurances of Fe-oxyhydroxide associated with high concentrations of Th, U and LREEs at great depths.
3) Recent trace element distribution in a reactivated crush zone.
4) Use of Ce-anomalies and Eu-anomlies for tracing REE migration paths.
5) Validation of laboratory measured K_d's on crushed granite and mineral separates by determining distribution coefficients between fracture coatings and corresponding groundwater ("in situ" K_d's).

The examination of the relation between "in situ" K_d's and laboratory-determined K_d's shows that the "in situ" K_d's are on average a factor of 100 higher for Sr, Cs, Co, Eu and about 10 for U.

It is suggested that fracture minerals such as Fe-oxyhydroxide, carbonates and clay minerals have sorption capacities significantly different from those of crushed granite. This is one of the explanations for the higher "in situ" K_d's compared with the laboratory-determined ones.

CONTENT

1. INTRODUCTION.....1

2. GEOLOGICAL SETTING.....3

3. SAMPLING.....8

3.1. Rock samples.....8

3.2. Fracture mineral samples.....8

3.3. Water samples.....10

4. ANALYSES AND RESULTS.....16

5. DISCUSSION.....25

5.1. Clay minerals formed by in situ weathering of granite and dolerite.....27

5.2. Hf-normalisation of trace elements in fracture fillings.....31

5.3. Studies of hematite/Fe-oxyhydroxide in fractures at great depth (>500 m vertical depth) and in near-surface fractures (<150 m).....32

5.4. A near-surface crush zone.....40

5.5. Ce and Eu-anomalies.....45

5.6 Distribution coefficients for fracture mineral/groundwater phases ("in situ K_d").....48

6. CONCLUSION.....67

7. REFERENCES.....69

In this report the boreholes are named KLn. The complete correct names used in the SKB database GEOTAB are KKLnm, i.e. KL2 = KKL02 etc.

1. INTRODUCTION

Predictions of future (up to 100 000 years) effects of contamination of the geological environment by radionuclides from an underground waste disposal site are based on the modelling of different processes responsible for the radionuclide migration. Some parameters used in model calculations, e.g. distribution coefficients, are usually determined in laboratory experiments. There is, however, a need for validation of the migration modelling as well as of the laboratory-based data.

Chapman et al. (1984) have thoroughly assessed validation involving comparison of the results of migration modelling with the results of "natural analogues", i.e. similar naturally occuring processes that mimic the complexity of events and varying geochemical conditions that can be expected during the long storage period. For the actinides Np, Pu, Am and Cm, which are not normally observed in nature, naturally occuring elements like Th, U and REE, are suggested as more or less suitable "chemical analogues" (Chapman et al., 1984). Natural analogue studies which mainly concern the mobilisation and transport of ore elements from well defined U, Th and REE deposits have also been reported (Smellie, 1984).

In the present work we have studied the behaviour of elements classified as chemical analogues (Th, U and REE) as well as certain additional major and trace elements (Fe, Na, Sr, Ba, Rb, Cs, Hf, Zr, Ta and Sc) in a crystalline (granitic) rock environment which is of interest for underground waste disposal. The main purposes of the work have been to:

- Study the mobilisation, migration and sorption processes (past and present) responsible for the present distribution of these elements in fracture filling minerals.
- Determine "in situ" distribution coefficients from analyses of fracture filling/groundwater pairs and compare them with laboratory-based data (parameter validation).
- Utilize the redox sensitivity of Ce and Eu to, if possible, trace REE pathways and determine past and present redox conditions.

The samples have been taken from the Klipperås study site in southern Sweden (Fig. 1), where extensive geological, geophysical and geochemical investigations have been carried out by SKB (Swedish Nuclear Fuel and Waste Management Co) in order to test the conditions for disposing high level radioactive waste (HLW) in crystalline rocks. Although this site does not fulfill all the requirements for a good natural analogue (as defined by Chapman et al. (1984)), we nevertheless believe that site-specific knowledge of migration parameters and processes relating to natural chemical analogues is necessary for a thorough assessment of the validity of predictions concerning radionuclide dispersal from a site.

The geophysical conditions at the Klipperås site have been described by Sehlstedt and Stenberg (1986), the hydrogeological conditions by Gentzschein (1986) and the geological and tectonic conditions by Olkiewicz and Stejskal (1986). The latter report also includes the results of a detailed core mapping. Studies of fracture fillings have been reported by Tullborg (1986). Groundwater from selected fracture zones has been sampled and analysed (Laurent, 1986). The relationship between hydrochemical conditions and hydrogeological conditions has been discussed by Smellie et al., (1987).

Consequently, the availability of a substantial body of data, core samples with fracture fillings and preserved groundwater samples made the Klipperås study site highly suitable for the present work.

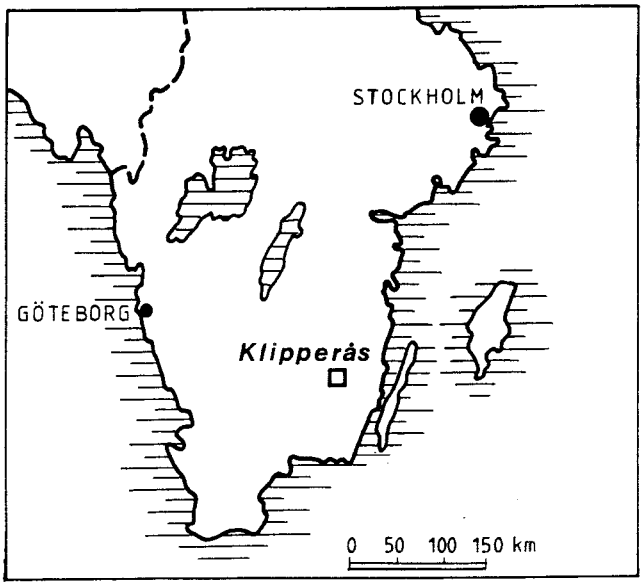

Figure 1. Location of the Klipperås study site.

2. GEOLOGICAL SETTING

The regional geology of the Klipperås area has previously been described by Holst (1879, 1893) and Åberg (1978). The region is dominated by granites (Småland-Värmland granites) and acid volcanics (Småland porphyry) which are postorogenic in relation to the Svecofennian orogeny. Datings of the Småland-Värmland granites have yielded ages between 1750 and 1650 Ma (Åberg, 1978; Aftalion, 1981). The Småland porphyries are suggested to be closely related to the plutonism (Persson, 1985) and have yielded a Rb-Sr age of 1645 Ma according to Åberg (1978).

A detailed description of the geology within the study site has been provided by Olkiewicz et al. (1984) and Olkiewicz & Stejskal (1986). The topography of the region is flat with an almost complete till cover, which makes geological interpretations uncertain. However, based on the drilling programme as well as geophysical interpretations a geological map of the study site has been compiled (Fig. 2). According to the core mapping 85% of the total core length is granite, 7% greenstone, 5.5% porphyry, 1.5% mafic dyke and 1% aplite.

Several generations of dykes have been found within the area, e.g composite dykes of porphyry, usually associated with uralitic basites. These dyke porphyries yield Rb/Sr ages of c. 1620 M.a., i.e. they are approximately similar in age to the Småland porphyries (Åberg, 1978). Different metabasites and basic volcanics are also present in the drill cores.

N-S to NE-SW-striking dolerites are represented in the area. These are suggested to be of Sveconorwegian age, 900 to 1000 M.a. (Patchett 1978).

Tectonically, the study site at Klipperås is characterized by several distinct zones, some of which accompany more or less vertical dykes of dolerite (Fig. 3). Most of the lineaments as indicated by geophysical and hydrogeological measurements are vertical to subvertical, although exceptions occur (e.g zone 4 which dips 65° to SE). One horizontal zone at a depth of 780 m in borehole Kl 2 has also been found.

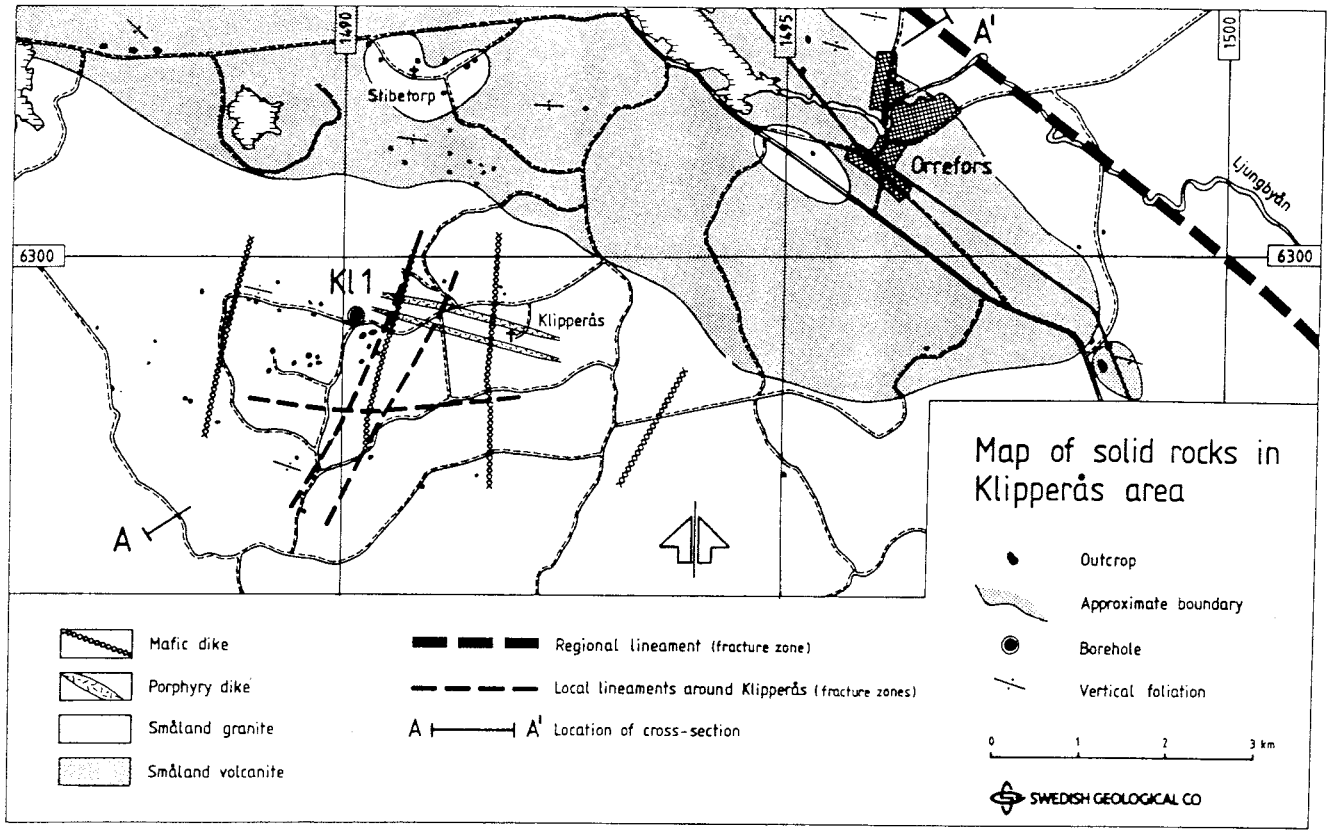

Figure 2A. Map of solid rocks in the Klipperås area (Olkiewicz & Stejskal 1986).

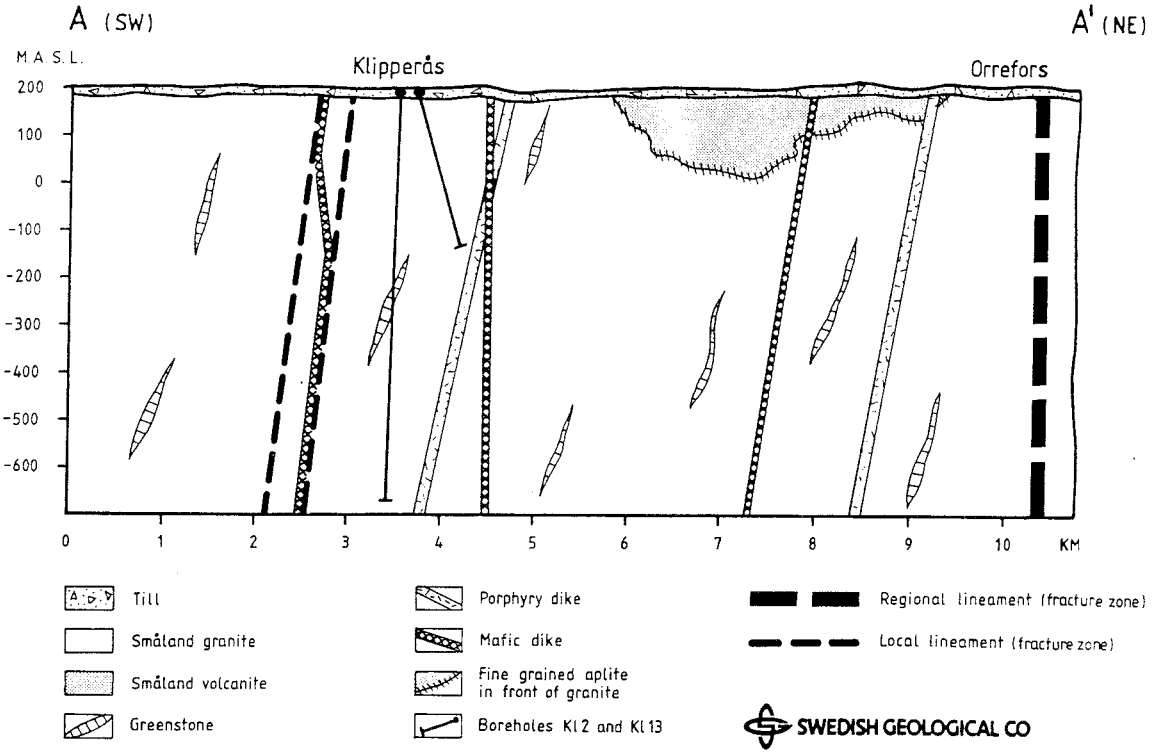

Figure 2B. Schematic vertical cross section of the Klipperås area (Olkiewicz & Stejskal, 1986).

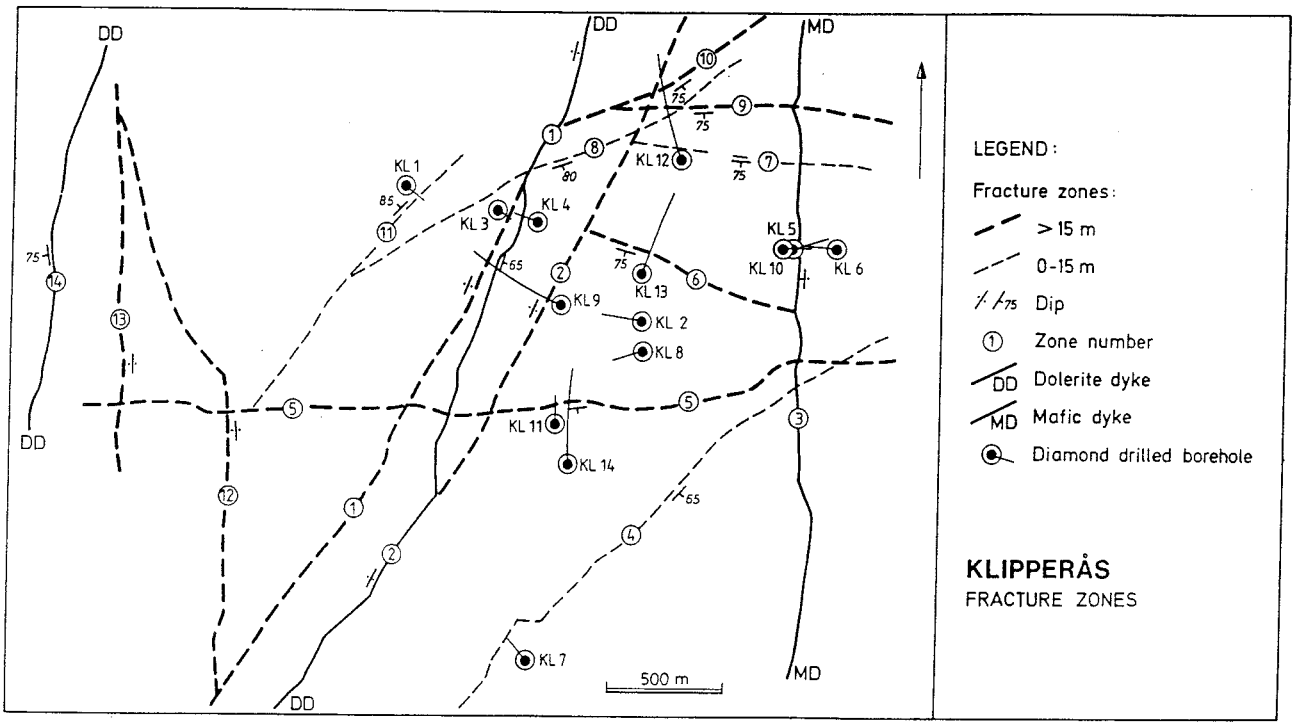

Figure 3. Locations of fracture zones and mafic dykes at the Klipperås study site (Olkiewicz & Stejskal, 1986). Boreholes Kl 1 and Kl 2 are subvertical whereas the others are inclined 60° to the surface.

Based on microscopy of drill core samples, the following sequence of tectonic events has been established (Tullborg, 1986) (cf. Table 1):

The oldest deformation (I in Table 1) that can be traced in the granite samples has resulted in dislocations within feldspar crystals and formation of subgrains in quartz crystals. Tullis and Yund (1977) found that the transition from mainly microfracturing to mainly dislocation in crystals occurs at 300-400°C for quartz and 550-650°C for feldspar at crustal depths exceeding 18 km. This makes it reasonable to assume that the deformation (I) took place at great depth and early in the history of the granite. The deformation phase (I) was followed by intrusion of the composite dykes of basites and porphyry and the first generation of quartz-sealed fractures.

The second event (II) represents a complex period with formation of hydrothermal minerals and extensive brecciation and mylonitisation. Two mineralisation sequences can be distinguished: (IIa), which is dominated by epidote and muscovite, and (IIb), which is characterised by adularia and hematite. As event (II) cannot be traced in the dolerite dykes (which are suggested to be of Jotnian age, Patchett, 1978) it probably took place before 1100 Ma.

The third event (III), which includes formation of the minerals chlorite, hematite and calcite, may be contemporary with, or later than, the intrusion of the dolerite dykes, as these minerals are found within most of the dykes. Similar dolerite dykes in the Karlshamn, Bräkne-Hoby and the Forserum regions have been dated to 871±25 - 1048±35 Ma (Rb-Sr age according to Patchett, 1978).

The last phase (IV) of fracture filling formation is still active resulting in precipitation of calcite, clay minerals and Fe-oxyhydroxide.

Hydrogeological investigations including water balance studies, groundwater Table recordings and water injection tests were reported by Gentzschein (1986). The water injection tests showed relatively high values of conductivity in the upper parts of the boreholes (10^{-9}m/s to 10^{-5}m/s). In general, high conductivity values were recorded down to 500 m, while below this depth there

is a dominance of values between 10^{-11}m/s and 10^{-9}m/s. The flat topography of the area suggests a low hydraulic gradient. This has also been confirmed by piezometric measurements in the boreholes. Except for one section the measured pressure difference was less than 5 m water column.

The water injection tests and an isotope investigation of calcites in fissure fillings (Tullborg, 1986) point to generally lower hydraulic conductivities in the basic dykes than within the granite itself.

Table 1. Sequence of tectonic events according to studies of thin sections. Figures I (oldest) to IV (youngest) indicate relative ages.

I)	a)	Dislocations in feldspars associated with formation of subgrains in quartz.
		- Intrusion of mafic and porphyry composite dykes (1620 Ma').
	b)	Quartz sealings in fractures
II)	a)	Epidote + Muscovite ± Calcite ± Quartz ± Chlorite (Mylonites)
	b)	Adularia + Hematite
		- Intrusion of dolerite dykes (875 to 1048 Ma")
III)		Calcite + Chlorite ± Hematite
IV)		Calcite + Clay minerals + Fe-oxyhydroxides

'Åberg (1978)
"Patchett (1978)

3. SAMPLING

Rock samples representative of the bedrock, different fracture filling samples and groundwater samples from selected fractures have been analysed.

3.1. Rock samples

Rock samples were taken from drill core Kl 9. Granite, which dominates the area, is represented by 7 samples, equally distributed between 20 and 720 m depth. Quartz porphyry, dolerite and greenstone rock types are represented by one sample each.

3.2. Fracture mineral samples

In the present study, the fracture filling samples have been subdivided into four main groups, some of which are associated with certain problems which were dealt with in previous works (e.g. Tullborg, 1989). The groups are:

a) Clay minerals formed in situ.
b) Hematite/Fe-oxyhydroxide in fractures/fracture zones at great depth (>500 m) and near-surface (<150 m).
c) A near-surface crush zone.
d) Groundwater/fracture filling pairs sampled for "in situ" K_d studies.

The depth positions (measured along the drill cores) of the analysed fracture fillings are marked in the figures 4 to 10 which show the variations with depth of hydraulic conductivity and frequencies of calcite and Fe-oxyhydroxide coated fractures in the investigated boreholes. (Hydraulic conductivity was not measured in Kl 7 and Kl 10 and Fe-oxyhydroxide was not mapped in cores Kl 1, Kl 2 and Kl 7)

The four groups of fracture filling samples are described in more detail below:

a) Three fractures dominated by clay minerals are represented by the following samples:

1) Almost pure muscovite/illite from a fracture in granite, where the illite is probably the result of weathering/alteration of the granite itself (Kl 10:21.70m).
2) Complex fillings dominated by muscovite/illite with some hematite/Fe-oxyhydroxide and chlorite. Fillings from two similar fractures are combined into one sample (Kl 12:21. 55+25.5 m).
3) Mixed-layer clay from a fracture in a dolerite dyke (Kl 9:373.9m).

b) In some cases Fe-oxyhydroxide (rust) has been observed at unusually great depths (Olkiewicz & Stejskal, 1986; Tullborg, 1986) e.g. in the hydraulically conductive zone at 600 to 650 m core length (Fig. 10). Fe-oxyhydroxide is also found in the uppermost part of the drill core. The near-surface rust (corresponding to a calcite depletion) is the result of recent day percolation of CO_2 saturated, oxidising water. At great depth, however, reducing conditions are most probable judging from the water chemistry (Smellie et al., 1987). Different processes are thus probably responsible for the rust production. In order to understand and describe the processes at great depth samples from the following levels of Kl 13 were investigated: 613.1m, 617.1m, 623.6m, 624.7m, 624.9m, 625.4m, 647.6m and 653.3m. For comparision two samples were collected from near-surface, water-conducting fractures which are coated with hematite, Fe-oxyhydroxide and chlorite (Kl 9:28.25 m and Kl 2:122.6 m).

c) There is a near-surface (100 m vertical depth) crush zone in Kl 7:125 m. The zone is defined by sharp-angled grains some of which are cemented together by Fe-oxyhydroxide. Microscopy of the grains shows that this zone originally consisted of a complex metabasic dyke and has been tectonically activated several times. The last activation caused a complete crushing of the material. The sparse sealing of the zone suggests a relatively late, possibly post-glacial reactivation of the zone. The fracture is

represented by two samples: Kl 7:125 m A (Fe-oxyhydroxide enriched) and Kl 7:125 m B (matrix).

d) An evaluation of the hydrochemical conditions in the Klipperås area (Smellie et al., 1987) revealed that three samples of groundwater can be regarded as representative (see below). Samples of fracture minerals that have been in equilibrium with these waters were carefully selected (based on e.g. core mapping and geophysical logs) in borehole Kl 1:440 m, Kl 2:329 m and Kl 9:699 m, respectively, in order to measure distribution coefficients.

3.3 Water samples

Groundwaters have previously been sampled from selected water-conducting zones using specially designed equipment for downhole sampling combined with immediate analyses of main constituents and redox-sensitive trace elements in a field laboratory. The selected zones were sealed off by packers and the waters were pumped directly into the field laboratory without any contact with the atmosphere. The field equipment is described by Almén et al. (1986) and the results of the water analyses are reported by Laurent (1986).

Smellie et al. (1987) presented a thorough evaluation of the water data and the hydrogeological measurements in order to define those water samples which are representative of the geochemical conditions in the sampled zone (e.g. free of contaminating drilling fluids). Three of these representative samples, which had been acidified and stored in polythene bottles at low temperatures, were re-analysed for trace element contents in the present study.

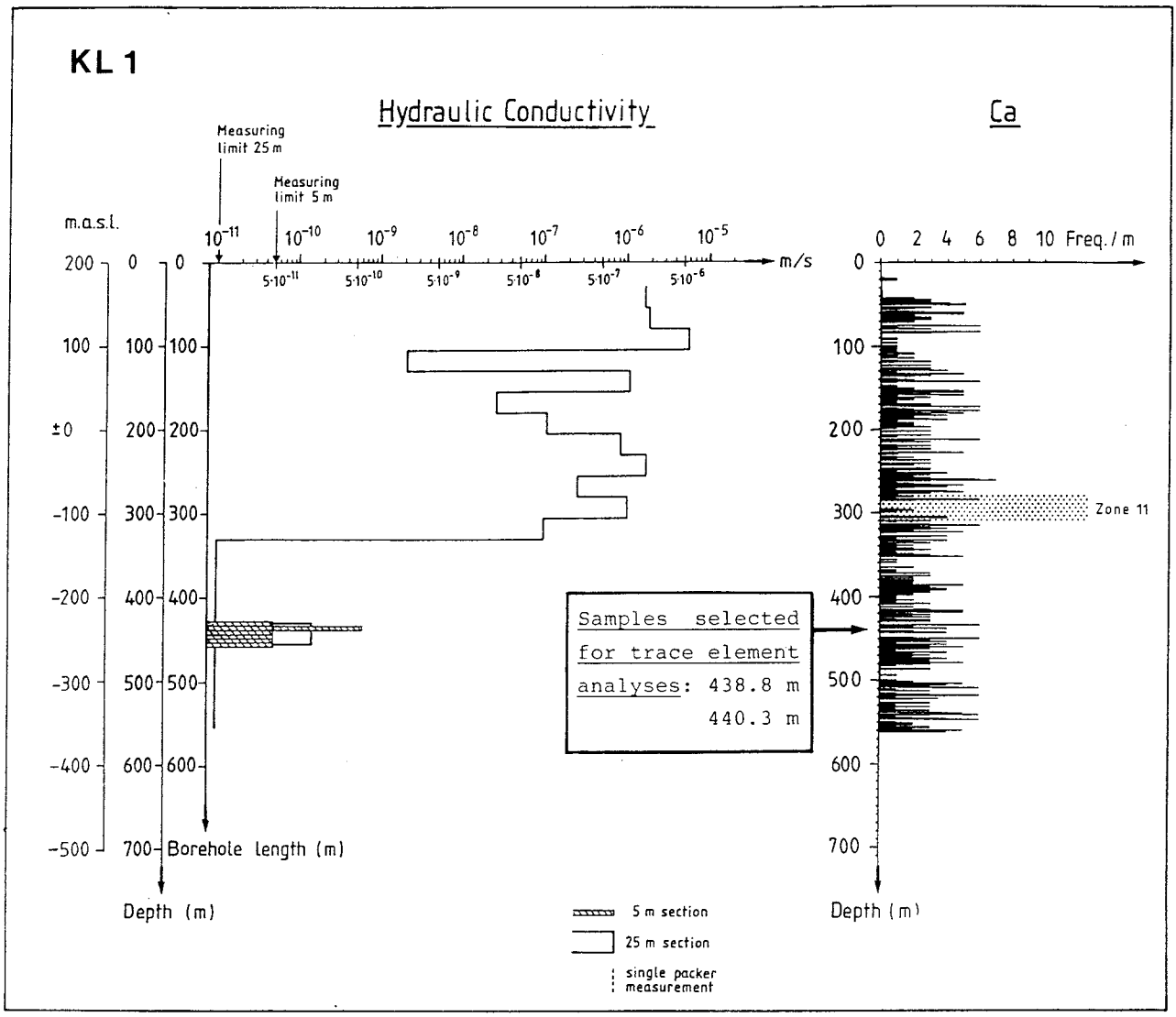

Figure 4. Hydraulic conductivity and frequency of calcite coated fractures (Ca) in drill core Kl 1.

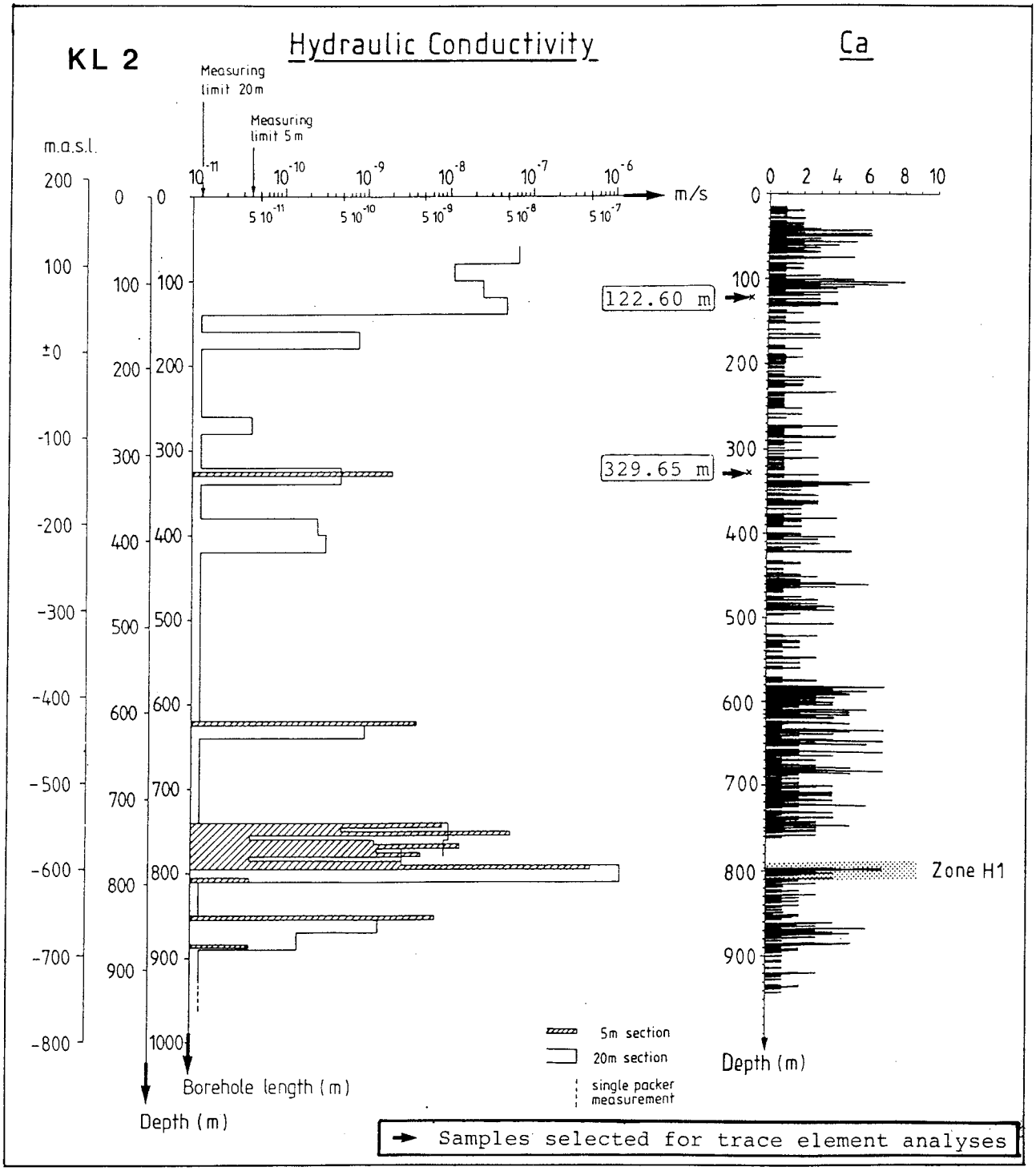

Figure 5. Hydraulic conductivity and frequency of calcite coated fractures in Kl 2.

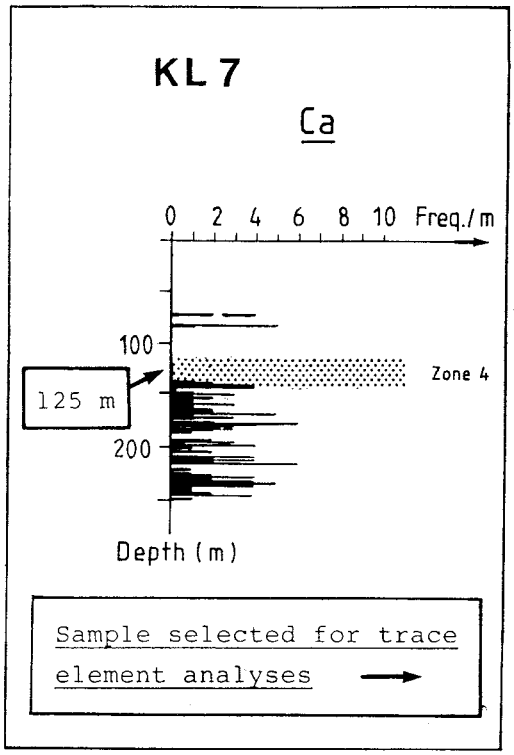

Figure 6.

Frequency of calcite coated fractures (Ca) in drill core Kl 7. Hydraulic conductivity have not been measured in this drillhole.

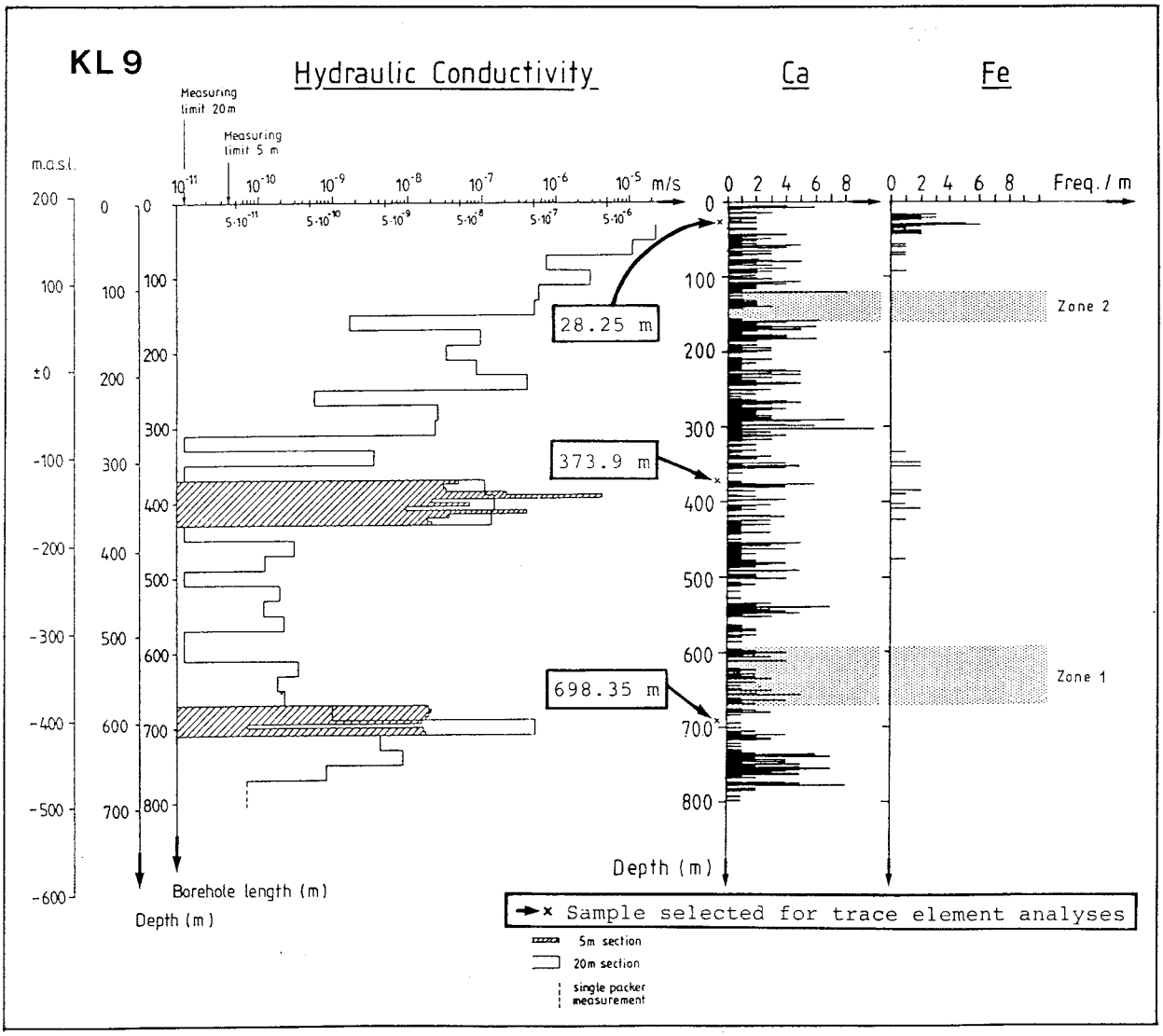

Figure 7. Hydraulic conductivity and frequency of calcite (Ca) and Fe-oxyhydroxide (Fe) coated fractures in Kl 9.

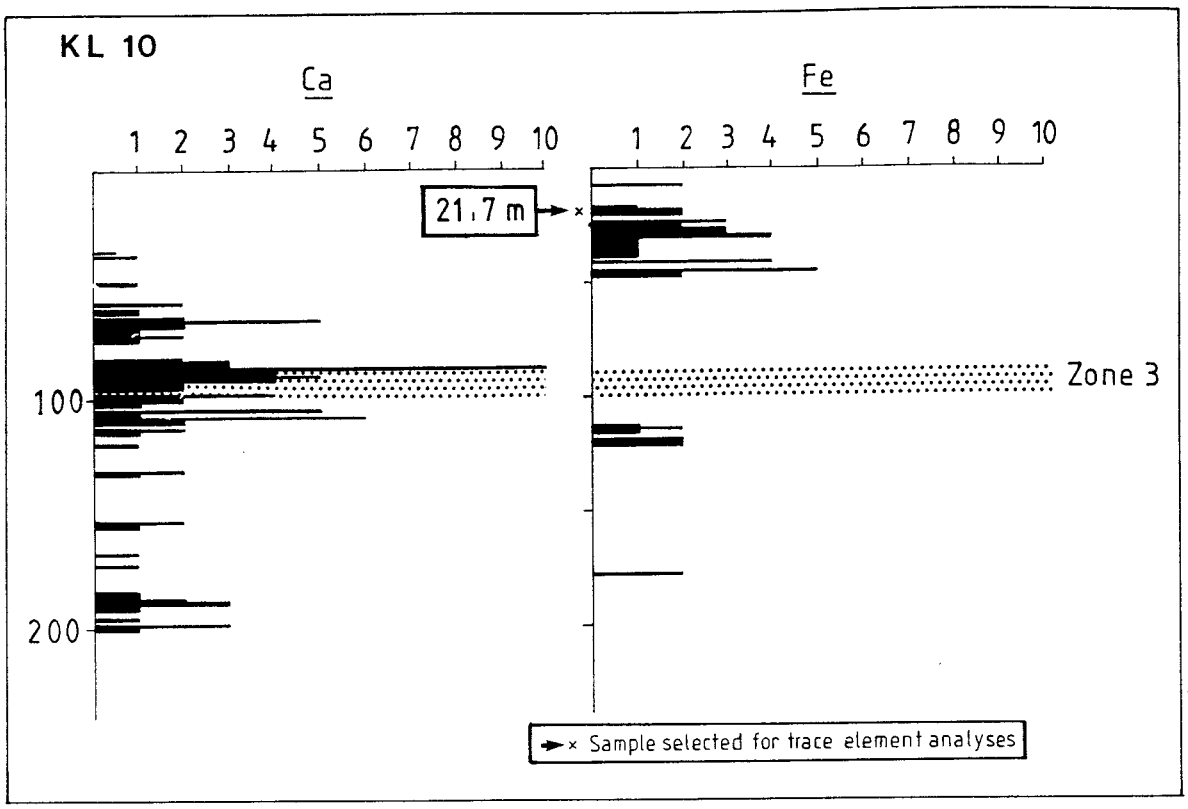

Figure 8. Frequency of calcite (Ca) and Fe-oxyhydroxide (Fe) coated fractures in Kl 10.

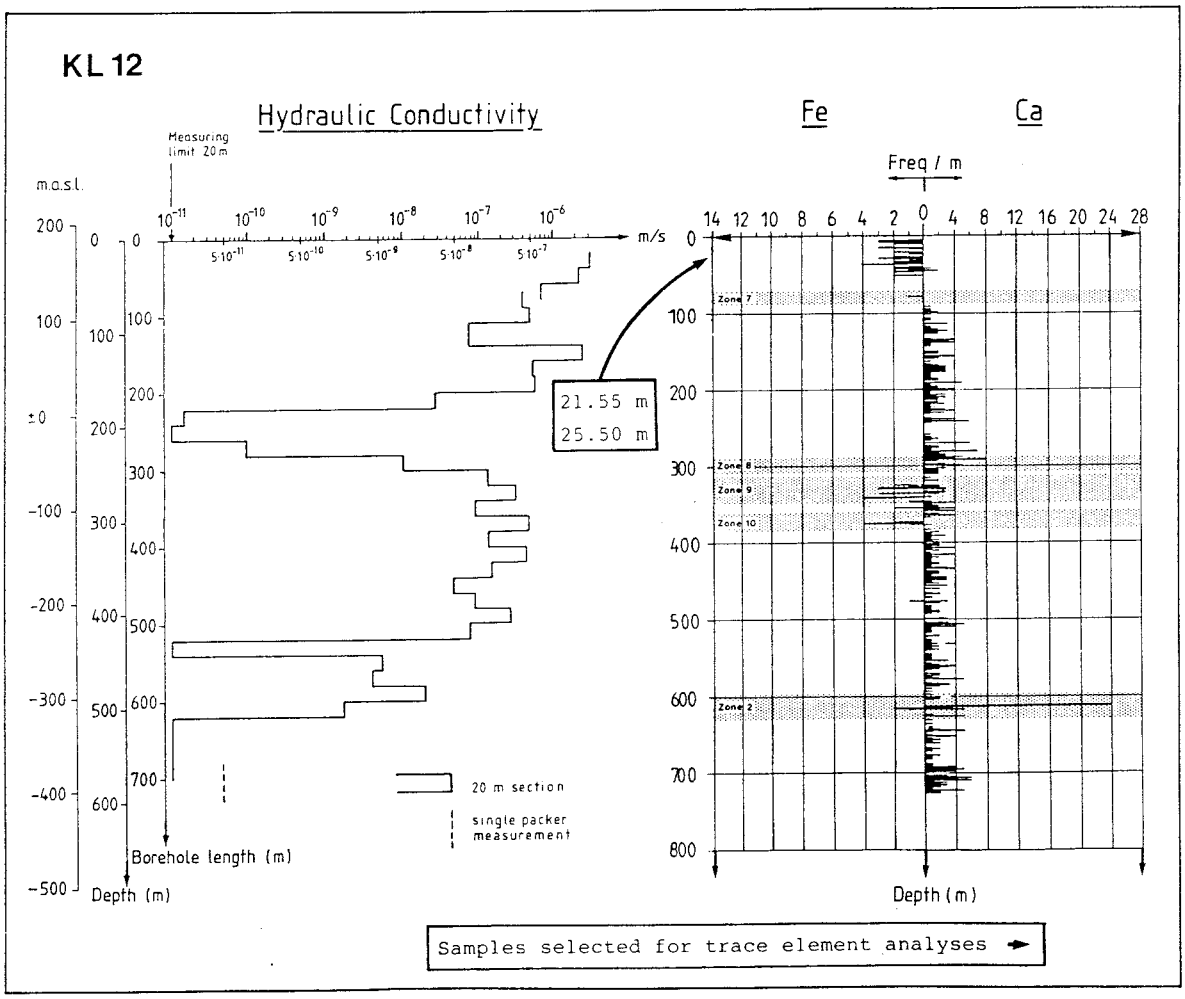

Figure 9. Hydraulic conductivity as well as frequency of calcite (Ca) and Fe-oxyhydroxide (Fe) coated fractures in Kl 12.

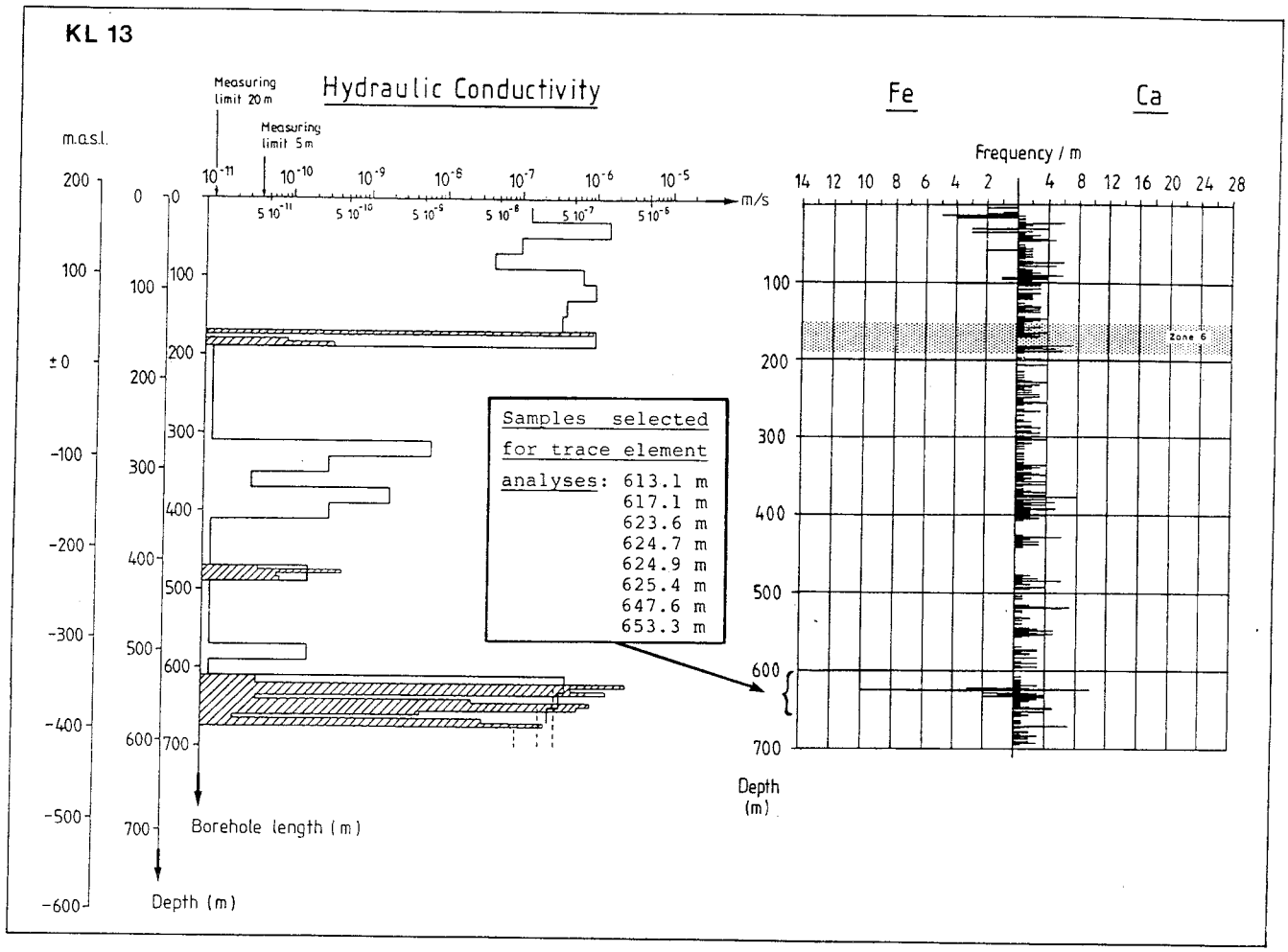

Figure 10. Hydraulic conductivity as well as frequency of calcite (Ca) and Fe-oxyhydroxide (Fe) coated fractures in Kl 13.

4. ANALYSES AND RESULTS

Different methods have been employed to identify the fracture mineral phases (XRD and microscopy) and analyse trace (INAA) and main elements (ICP-AES). As limited amounts of the fracture filling samples were available it has not been possible to apply all methods to every sample. The analyses carried out for each sample are shown in Table 2. The methods of analysis are described in the following.

For XRD the fracture coatings were scraped off the wall rock surface with either a plastic or a steel knife. The samples were ground and the powder smeared out on glass slides (so called semi-orientated mounts). The XRD analyses were performed using Cu Kα radiation, 50 W and 30 mA. Clay minerals were indentified by routine methods i.e. position of basal reflections and response to ethylene glycol treatment. The analyses were performed at different laboratories (SGAB in Luleå, Department of Geology, University of Gothenburg and SGU in Uppsala) and on different occasions. However, the same techniques were used and the results (shown in Table 3) are therefore comparable.

As a complement to the mineral identification, thin sections, perpendicular to the fracture edge, were prepared from the Fe-oxyhydroxide zone in Kl 13: 610-650 m. The results of microscopy of the thin sections are presented in Table 4, which shows the relative ages of the minerals present in the fractures.

Main and trace elements of the rock samples and the clay sample Kl 10:21.70 m were analysed using plasma technique (ICP-AES) at SGAB in Luleå. The samples were mixed with lithium metaborate, melted and dissolved in HNO_3 before being analysed. The precision of the analyses is 1.5% RSD (relative standard deviation).

Instrumental neutron activation analysis (INAA) was employed for element determinations in samples of rock, fracture filling and groundwater. About 100 to 200 mg of rock samples, 10 to 200 mg of fracture filling samples (depending on the available amount of material) and 1-2 litres of the water samples (concentrated by evaporation) were irradiated in an integrated neutron flux of 10^{16} - 10^{17} n/cm^2 and subsequently measured for gamma ray

activities. Standard solutions and reference rock samples were used for calibration and USGS standards (mostly BCR, G-2 and GSP-1) for checking accuracy.

The precision of the rock and fracture filling analyses, as determined from repeated analyses of an internal rock standard is 5 to 10 % for most elements (Na, Fe, Cr, Co, Ba, Rb, Cs, Hf, Th, U, Sc and REE). Lower precision, 10 to 20 % was obtained for Sr Zr, Gd, Sb and Zn. The precision of the water analyses for most elements is 10 to 20 % but considerably lower, 50 %, for REE and Sc. The latter is due to the generally low concentrations of REE and, in particular, to the high U/REE ratio in these waters which caused problems in correcting for La, Ce, Nd and Sm fission products.

The rock samples were prepared in an agate mill, whereas the fracture fillings were only slightly homogenized in an agate mortar. As mentioned above, some fracture coatings had to be removed from the fracture surfaces using a steel knife. The risk of contaminating the sample with alloying elements from the steel was controlled by comparative analyses of twin samples - one removed with a plastic and one with a steel knife - from two fracture surfaces. When a fairly soft mixed-layer clay was sampled (Kl 9:373.9 m), no contamination from the steel knife was observed. The other fracture surface sampled (Kl 9:28.25m) had to be scraped much more intensely due to the fracture mineral composition (hematite and chlorite), resulting in a marked contamination of the "steel knife sample" with Cr and, to a lesser extent, with Fe. Higher Hf and slightly higher Yb and Lu concentrations were also found in the "steel knife sample", probably due to the removal of more zircon minerals from the wall rock. A more intense scraping with e.g. a steel knife may thus release and add to the sample minerals from the more or less altered wall rock surface. To correct for this effect, Ti and Hf normalisation was employed (see section 5).

The results of the chemical analyses are shown in Tables 5 (rock types), 6 (fracture fillings) and 7 (groundwaters).

Table 2: Fracture filling samples selected for analyses

SAMPLE	ANALYSIS
Kl 1: 438.80*	XRD, INAA
Kl 1: 440.30*	XRD, INAA
Kl 2: 122.60	INAA
Kl 2: 329.65*	XRD, INAA
Kl 7: 125	T, INAA
Kl 9: 28.25	INAA
KL 9: 373.9	XRD, INAA
Kl 9: 698.35*	XRD, INAA
Kl 10: 21.70	XRD, INAA
Kl 12: 21.55+25.5	XRD, INAA
Kl 13: 613.1'	T, XRD, INAA
Kl 13: 617.1'	T, XRD, INAA
Kl 13: 623.6'	T, XRD, INAA
Kl 13: 624.7'	T, XRD, INAA
Kl 13: 624.9'	T, XRD, INAA
Kl 13: 625.4'	T, INAA
Kl 13: 647.6'	T, XRD, INAA
Kl 13: 653.3'	T, INAA

T = thin section for microscopy
XRD = X-ray diffractometry
INAA = Instrumental neutron activation analysis

* = Fracture filling sample corresponding to section sampled for groundwater
' = Fracture filling samples from Fe-oxyhydroxide/hematite bearing zone

Table 3. X-ray diffractometry of fracture coating samples.

Sample	Chl	Ca	Si	Qz	Ep	Mu/Il	Hm	Py	Goe	Kaol	M-l.cl	Gi	Pl	Kfsp
Kl 1:438.80				I		III								III
Kl 1:440.30		II		I		III	II							I
Kl 2:329.65	II	III		II		III				I		I?		I
Kl 9:318.90											III			
Kl 9:698.35			I	I	III				I			I		I?
Kl I0:21.70						III								
Kl 12:21.55	I			II		III	I		I				II	III
Kl 12:25.50	II			II		III	I		I				I	III
Kl 13:613.1	I			II		III	II	I					I	III
Kl 13:617.6	II					II	I						II	II
Kl 13:623.6	I	I		II	I		I		III				II	I
Kl 13:624.7	I			III	I		I	I	I				II	I
Kl 13:624.9	III			III	I		II		II				II	I
Kl 13:647.6	I			II	I		II	I	II					III

Chl=Chlorite, Ca=Calcite, Si=Siderite, Qz=Quarz, Ep=Epidote, Mu/Il=Muscovite/Illite, Hm=Hematite, Py=Pyrite, Goe=Goethite, Kaol=Kaolinite, M-l.cl=Mixed-layer clay, Gi=Gibbsite, Pl=Plagioclase, Kfsp=K-feldspar.

III=dominating mineral in the sample, II=frequent, I=less frequent, I?=probably present

Table 4. Results of microscopy of fracture coatings

Sample	Ca	Chl	Qz	Ep	Py	Ad	Hm	G
Kl 13:613.1		3				1	2	
Kl 13:617.6		2					1	
Kl 13:623.6	3		1	2			3	
Kl 13:624.7	1				2	1	1	
Kl 13:624.9	1	1				1	1	2
Kl 13:625.4	3	4	1			2	2	4
Kl 13:647.6		2		1			1,2	
Kl 13:653.6	1,2,3			1	3	1	1	3

Ca=Calcite, Chl=Chlorite, Qz=Quartz, Ep=Epidote, Py=Pyrite, Ad=Adularia, Hm=Hematite, Goe=Goethite

1,2,3=relative age of mineralisation where 1 is the oldest

Table 5. Chemical composition of main rock types from Klipperås

Element	Granite average*	St.d.	Quartz porphyry	Greenstone	Dolerite
SiO_2 %	74.6	3.07		47.4	49.5
TiO_2	0.28	0.023	0.19	1.3	2.7
Al_2O_3	12.7	0.32	10.9	15.4	15.5
Fe_2O_3	1.8	0.21	1.0	11.9	10.4
MnO	0.051	0.0053	0.038	0.21	0.14
MgO	0.47	0.076	0.13	7.1	4.7
CaO	1.3	0.18	0.46	8.5	6.5
Na_2O	3.5	0.58	3.4	0.50	3.3
K_2O	4.7	0.43	4.5	0.51	1.2
Li ppm	8	1.7	5	48	11
Rb	139	32	161	-	-
Be	2.3	0.45	4	2	<1
Sr	223	24	41	650	490
Ba	735	108	320	120	540
Cs	0.70	0.26	0.43	1.0	2.3
Cr	3.7	0.40	4.2	76	41
Co	2.5	0.57	1.6	46	43
Ni	4	0.76	5	88	59
Cu	11	3.8	11	60	25
Zn	40	5.3	37	155	128
Sb	<0.5	-	<2	-	-
As	<3	-	-	-	-
V	20	2.2	9	243	184
Sn	4	0.5	6	<2	3
W	<2	-	<2	<2	<2
Pb	34	3.9	55	41	27
Zr	175	-	260	55	193
Hf	5.2	0.45	8.0	3.2	5.4
Ta	1.3	0.1	2.3	0.69	1.1
Th	22.2	3.2	26.6	0.81	1.4
U	6.7	2.3	10	0.87	0.57
Sc	4.0	0.48	2.1	35	21
Y	16	1.2	46	19	29
La	53	10	55	20	24
Ce	95	15	121	51	60
Nd	34	3	43	27	43
Sm	5.3	0.65	9.2	6.6	8.9
Eu	0.80	0.1	0.38	1.8	2.5
Gd	4.0	0.84	8.4	6.4	8.6
Tb	0.61	0.03	1.3	0.93	1.5
Yb	2.3	0.26	5.8	2.2	3.3
Lu	0.35	0.038	0.82	0.34	0.53

*=Average of seven samples, except for SiO_2 (three samples only)

Table 6. INAA results for fracture coatings and infillings

Element	Kl 1 438.80 m	Kl 1 440.30 m	Kl 2 122.60 m	Kl 2 329.65 m	Kl 7 125 m a)	Kl 7 125 m b)	Kl 9 28.25 m	Kl 9 373.9 m	Kl 9 698.35 m	Kl 10 21.70 m
Na %	3.4	1.6	1.1	0.72	1.0	0.77	0.76	0.084	2	0.087
Fe %	3.5	5.5	7.0	6.1	16.7	3.8	6.4	16.8	7.5	3.4
Cr ppm	-	-	-	-	340	183	27	4.3	-	6.5
Co	5.5	10.7	14.7	16	46	23	16.5	11.4	4.8	5.8
Zn	51	-	-	290	930	970	100	50	-	250
Sb	1	1	-	1	4.2	3.1	-	0.1	-	5.7
As	-	-	-	-	43		-	-	-	4
Rb	435	660	139	285	180	140	256	50	109	360
Sr	290	-	-	600	146	-	-	130	1330	-
Ba	1670	1500	1400	1380	730	630	-	145	410	1480
Cs	3.6	11.6	10.9	560	5.9	4.0	4.7	2.9	1.9	27
Zr	-	-	-	-	62	92	-	-	250	-
Hf	12.6	27.8	5.0	3	2.7	2.5	6.5	0.17	6.7	9.2
Ta	3.9	3.2	1.0	0.9	0.67	0.59	1	0.05	0.6	2.1
Th	53.9	148	37.2	13.5	3.0	3.9	220	0.29	55.7	42.0
U	236	383	72	44	16.8	8.9	123	0.28	55.8	37.2
Sc	11.4	24.2	12.8	6.4	10.8	9.4	10.5	1.1	24.4	10.8
La	756	2476	468	548	24.3	22.5	1021	1.2	1486	134
Ce	152	900	856	683	50	47	1091	1.8	1710	265
Nd	39	185	251	168	28	20	425	-	573	96
Sm	5.3	23.5	31.4	16.2	6.2	4.3	57.5	0.23	57.9	16
Eu	1.1	4.2	3.1	1.9	1.4	1.2	7.9	0.16	4.9	2.2
Gd	-	-	-	-	5.2	3.5	-	-	-	8.5
Tb	1.1	3.6	1.3	1.3	0.79	0.60	5.4	0.05	2.1	1.4
Yb	7.6	18	2.4	1.9	2.5	1.5	9.4	0.29	5.2	5.4
Lu	1.5	3.4	0.3	0.28	0.32	0.25	1.4	0.043	0.82	0.96

a) only grains cemented together with FeOOH

b) only single grains

Table 6. Continued

	Kl 12 21.55 - 25.5 m	Kl 13 613.1 m	Kl 13 617.1 m	Kl 13 623.6 m	Kl 13 624.7 m	Kl 13 624.9 m	Kl 13 625.4 m	Kl 13 625.4 m Calcite-enriched	Kl 13 647.6 m	Kl 13 653.3 m	Kl 13 653.3 m Calcite-enriched
Na %	1.5	1.5	1.4	1.5	0.7	0.82	0.14	0.056	1.7	0.22	-
Fe %	4.6	10.7	19.7	6.3	8.8	13.0	3.8	1.7	11.1	11.5	1.6
Cr ppm	8.5	-	-	-	-	-	-	-	-	-	-
Co	3.2	26	27	8.2	9.7	37	1.9	0.75	9.7	1	1.0
Zn	140	485	256	51	75	385	50	51	60	50	10
Sb	3.0	-	-	-	-	1	-	-	-	-	0.6
As	-	-	-	-	-	-	-	-	-	-	-
Rb	436	942	370	186	315	153	143	70	550	40	20
Sr		-	-	1000	-	-	-	-	-	-	-
Ba		6990	3035	500	750	500	500	200	750	500	100
Cs	10.6	14.4	3.7	3.1	3	3.3	2.6	1	25	1	1
Zr		-	-	-	-	190	200	-	-	-	-
Hf	6.5	1.6	4.8	5.2	5.2	5.3	2.9	0.58	4.4	2.0	0.5
Ta	2.1	1	2.1	1.3	2	1.0	1	0.25	2.1	0.5	0.2
Th	45.6	2.6	11.8	71.0	307	211	53.8	11.2	70.8	17.1	1.5
U	106	16.9	37	102	182	103	120	49	203	400	143
Sc	13.2	3.1	11.4	10.1	19.5	17.4	10.0	2.8	21.2	7.8	10.1
La	271	27	122	3243	4449	2245	1065	113	1281	942	179
Ce	451	36	158	3946	5726	2735	1374	129	1781	1341	283
Nd	173	13	47	1019	1462	766	358	35	510	432	107
Sm	20.9	1.5	5.1	97	165	83	36.9	3.8	51	57	18
Eu	2.4	0.28	0.93	16.2	26.5	14.4	7.1	0.70	7.4	9.3	2.5
Gd	10.9	-	-	-	-	-	-	-	-	-	-
Tb	1.8	0.25	0.71	5.1	9.8	4.3	2.4	0.39	2.9	4.3	2.4
Yb	6.2	0.72	2.1	6.0	9.3	4.4	3.2	0.73	3.6	11.3	12.4
Lu	1.2	0.12	0.33	0.91	1.1	0.85	0.46	0.10	0.56	1.7	2.1

Table 7a. Main and trace elements in groundwater from Klipperås (neutron activation analyses).

Element		Kl 1:406 m	Kl 2:329 m	Kl 9:696 m	Average*
Na	mg/l	46.5	40	17.5	
Ca		17	42	33	
Fe		0.011	0.14	0.11	
Rb	µg/l	3.5	4.3	4.9	4.2
Sr		296	267	313	292
Cs		0.07	0.093	0.10	0.088
Ba		53	134	91	93
Co		0.027	0.076	0.02	0.041
Cr		<0.17	<0.3	-	-
Zn		7.5	6.9	2.9	5.8
Sb		0.2	0.017	0.02	-
Hf		-	0.01	-	-
Th		<0.02	<0.02	<0.02	-
U		3.2	4.6	0.66	2.8
Sc		0.004	0.0032	0.0032	0.0034
La		<0.013	0.11	<0.13	0.11
Ce		0.25	0.24	0.25	0.25
Nd		-	-	-	-
Sm		-	0.033	-	0.033
Eu		0.0025	0.0021	0.0035	0.0027
Tb		<0.015	0.0073	-	0.0073
Yb		<0.050	0.024	<0.014	0.024
Lu		0.0028	0.0023	0.0032	0.0028
Ta		-	<0.02	-	-

Table 7b. Main element analyses in the groundwater from Klipperås (Smellie et al., 1987)

Na	mg/l	47	29	15
K		1.0	1.1	1.3
Ca		14	31	29
Mg		2.3	1.0	3.0
HCO_3		80	140	120
Cl		45	17	5.9
F		3.8	2.9	3.0
SO_4		1.5	0.1	4.3
Si		4.4	7.6	9.9
TOC		3.7	2.0	1.2
pH		8.3	7.6	7.6

* Average used in estimations of K_d for fracture zones from which water was not sampled.

5. DISCUSSION

In the following interpretations trace element distributions in fracture fillings are compared with those of rock samples representative of the host rocks.

Most of the investigated fractures occur in the granite and seven granite samples were analysed with average values given in Table 5. Typically of post-orogenic granites Th (22 ppm) and U (6.7 ppm) are fairly high. The REE pattern (Fig. 11) is fractionated in the LREE and exhibits a negative Eu anomaly ($Eu/Eu^* = 0.55$). The Zr/Hf ratio is "normal", c. 34.

The quartz porphyry is also high in Th (26.6 ppm) and U (10 ppm) but differs from the granite in e.g. Sr and Ba (which are lower in the quartz porphyry), and in the REE pattern (Fig. 11) which is characterised by a very pronounced negative Eu anomaly ($Eu/Eu^* = 0.14$) and higher concentrations of the HREEs.

The element concentrations are rather similar in the greenstone and dolerite samples, except for differences in the alkalies and calcalkalies, reflecting different An-content in the plagioclase. Both REE patterns (Fig. 11) have the signature of mafic rocks i.e. rather flat and without any Eu anomaly.

In order to illustrate the significance of chemical analogue distributions in fracture fillings to predictions of actinide migration, the following discussion is subdivided into sections dealing with relevant problems:

1) Redistribution of elements in connection to clay forming alteration processes and preferential sorption of elements on clay minerals.
2) Occurances of Fe-oxyhydroxide associated with high concentrations of Th, U and La (and strongly fractionated REEs) at great depths.
3) Recent trace element distribution in a reactivated crush zone.
4) Use of Ce-anomalies and Eu-anomlies for tracing REE migration paths.
5) Validation of laboratory measured K_d's by determining distribution coefficients between fracture coatings and corresponding groundwater ("in situ" K_d).

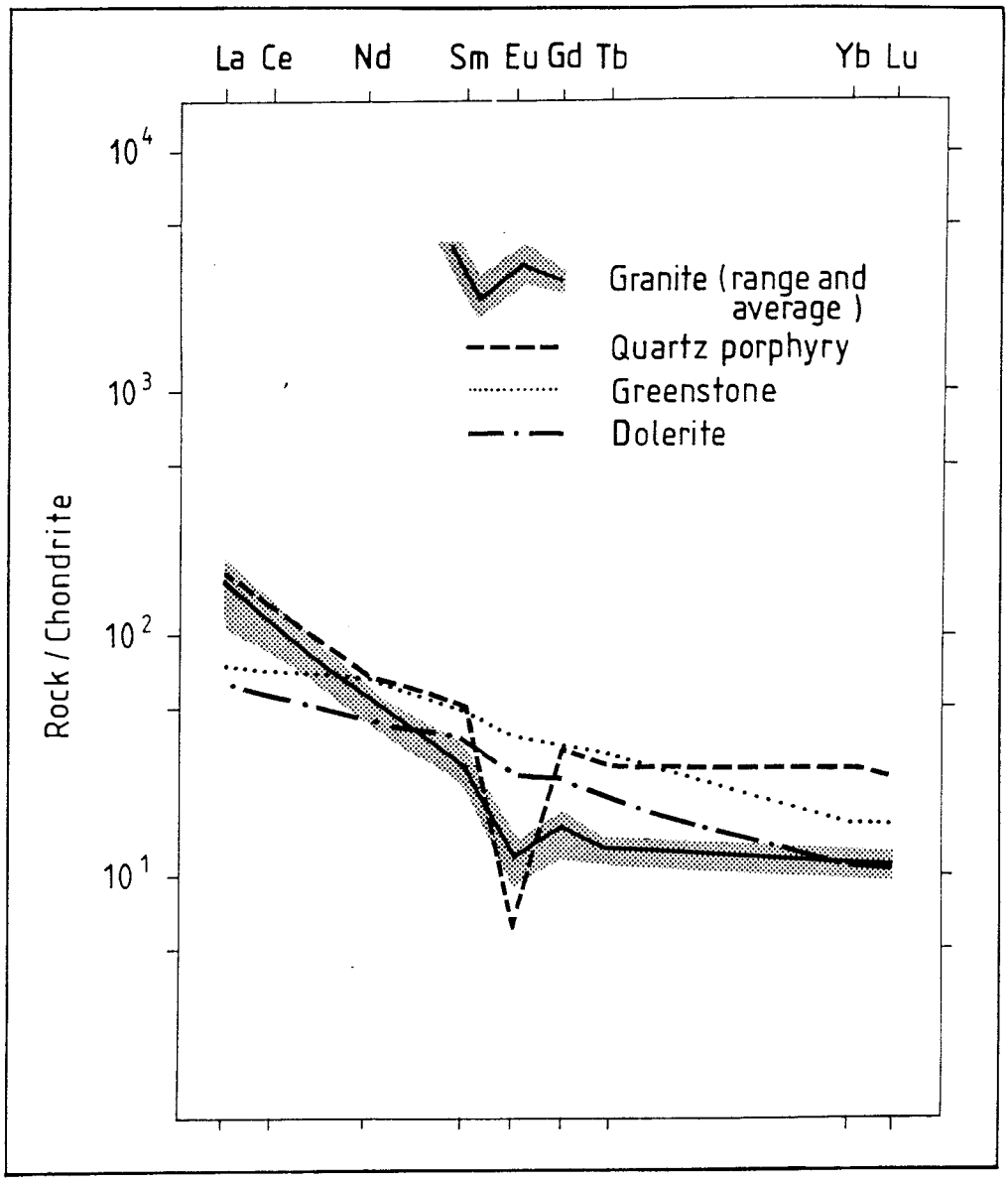

Figure 11. Chondrite-normalised REE curves for the common rock types in the Klipperås area.

5.1 Clay minerals formed by in situ weathering of granite and dolerite

Two samples of pure clay minerals (which are probably products of in situ weathering) were studied in order to elucidate the influence of clay alteration on the trace element distribution. The analysed fracture fillings are:

- one muscovite/illite filling from a water-conducting fracture in granite (Kl 10:21.70 m)
- one mixed-layer clay from a fracture in a dolerite dyke (Kl 9, 373.9m).

The gain and loss of elements in connection with the alteration process was estimated for the muscovite/illite sample by means of the immobile element method (Nesbitt, 1979). Ti was assumed to be an immobile element (reasons for using Ti are discussed by e.g. Nesbitt (1979) and Middelburg (1988)) and the concentration values were recalculated according to the formula given in Fig. 12. These Ti-normalised values are compared with those of the "average" granite (cf. Table 5) assumed to be representative of the parent rock. The possibility of slight differences in composition between the granite average and the parent granite can, however, not be ruled out. A ratio of one in Figure 12 means that the element has been immobile, relative to Ti, during the alteration process; a ratio >1 means gain of the element and a ratio <1 means loss of the element.

Of the alkalis and the alkaline earths, Na, Ca, K and Sr show ratios less than one, i.e. these elements were partly removed from the system as dissolved species in the groundwater. The large ions Ba, Rb and Cs show ratios greater than one, indicating uptake from the groundwater by sorption or ion exchange.

The apparent immobility of Zr, Hf, Ta and Th (with ratios close to one) is interesting. Most Zr and Hf resides in zircon, a mineral which is very resistant to weathering. Th and probably also Ta are mainly hosted in accessory minerals which, like zircon, have been resistant to weathering. In principle, Zr or Hf can thus be used as the immobile element in assessing gain and loss of elements during weathering. They are, however, less uniformly distributed as compared to Ti (Nesbitt, 1979).

The reason for the strong enrichment of Cu, Zn and apparently

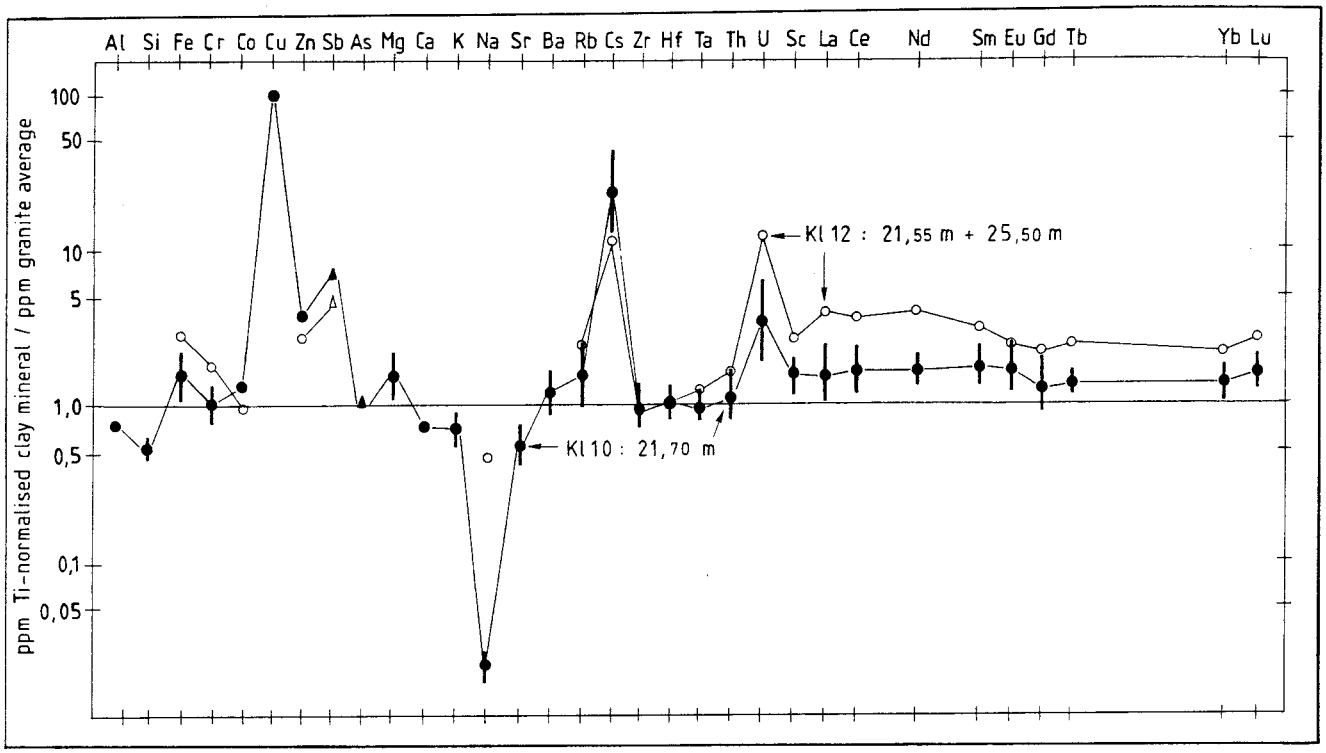

Figure 12. Ti-normalised trace element distribution pattern for sample Kl 10:21.7 m (illite/muscovite), solid circle, and Hf-normalised trace element pattern for sample Kl 12:21.55 and 25.5 m, open circle. The trace element contents of the sample (C_s) are normalised according to the formula:

$$C_{corr} = C_s \times A_{granite}/A_s$$

Where A can be Hf (Hf-normalisation) or Ti (Ti-normalisation).

also Sb is not clear. Middelburg et al. (1988) also found enrichments, relative to Ti, of Cu and Zn in alteration products and explained this as being due to oxidation of sulphide phases. Cu, Zn, As and Fe are then released and trapped in Fe-oxyhydroxide precipitates. This is also a possible explanation for the enrichment of Cu, Zn and Sb in the illite sample (Kl 10:21.70m) from Klipperås. Another explanation may be the presence of remnants of sulphides from the parent rock.

Both Al and Si are depleted in the clay and no change is observed for chromium.

Uranium is significantly enriched, probably by precipitation/sorption from inflowing groundwater. It is uncertain whether the slight enrichment of Sc and REE is significant or simply due to higher concentrations of these elements in the parent rock than in the granite average used for normalisation. The REEs are not significantly fractionated relative to the granite average (Figs. 12 and 13).

In conclusion, the gain (by sorption and ion exchange processes) of Cs, U, Cu, Zn and possibly Rb from the groundwater is significant, whereas the gain of e.g. Fe, Mg, Co, Ba, Sc and REE is somewhat uncertain due to a possible difference in composition between the granite average used for normalisation and the parent rock.

For the sake of comparison, a sample (Kl 12:21.55+25.5 m) consisting of not only illite/muscovite (although these minerals dominate) but also hematite/Fe-oxyhydroxide and chlorite is plotted in the same diagram (Fig. 12) as the pure illite/muscovite filling (Kl 10:21.70 m). As Ti was not analysed in this sample, Hf was used for normalisation. The two samples from the two different water-conducting, near-surface fractures, show largely similar trace element patterns, although some interesting differences are observed (Figs. 12 and 13):

- The Fe, U and REE gains are higher and the light REE/heavy REE ratio is slightly higher in sample Kl 12:21.55+25.5 m. U and REE (especially the light REE) are probably sorbed (or co-precipitated) on the hematite/Fe-oxyhydroxide phases. This is in agreement with general trends observed in other Fe-oxyhydroxide/hematite bearing fractures in the area.

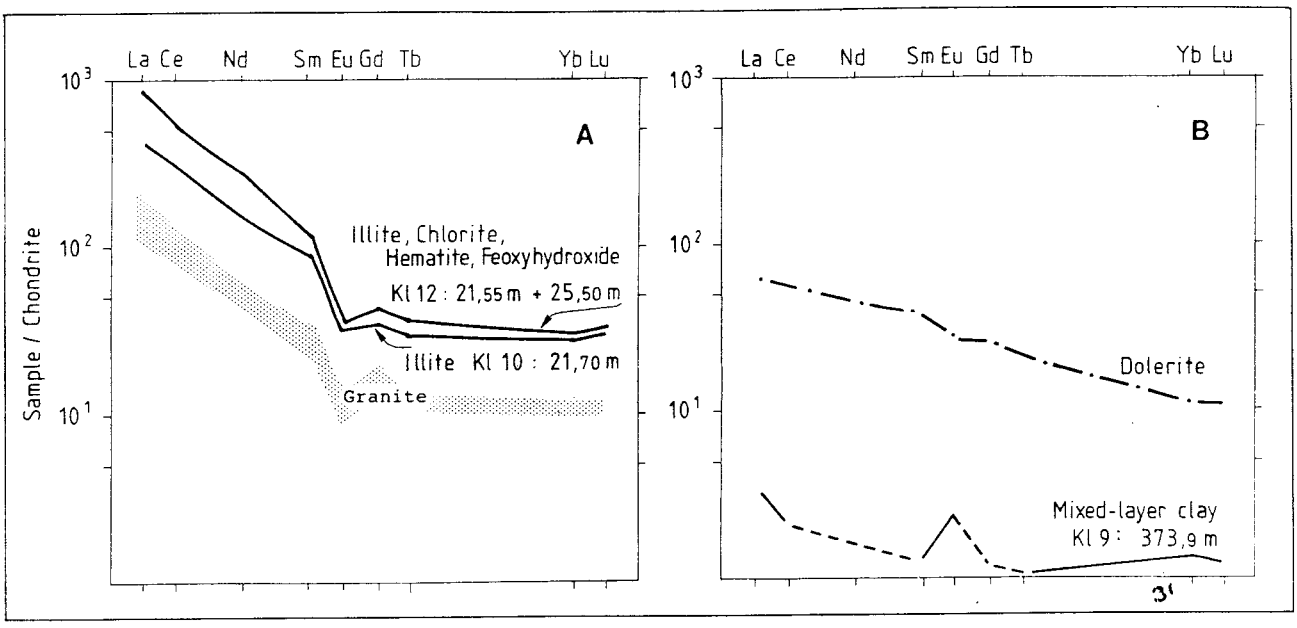

Figure 13. Chondrite-normalised REE curves of illite/muscovite dominated fracture samples and host granite (A) and mixed-layer clay and corresponding host dolerite (B).

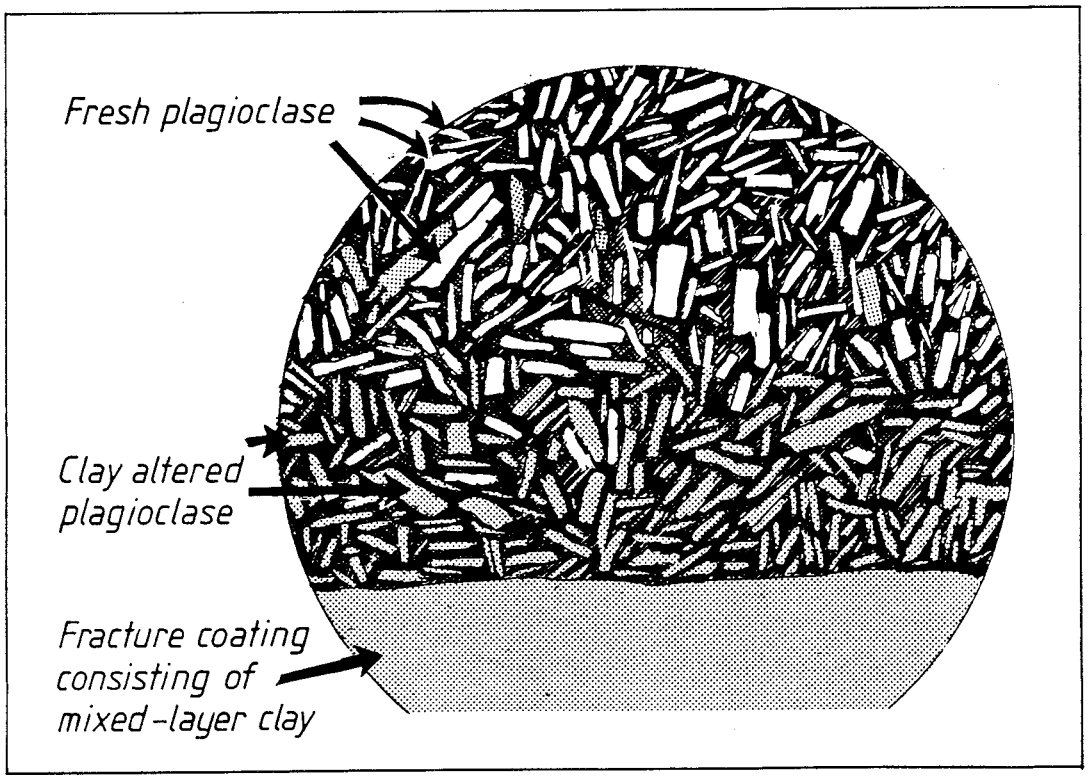

Figure 14. Sketch showing increasing alteration of plagioclase from the host dolerite towards the fracture edge in sample Kl 9:373.9 m.

- The Cs content is somewhat lower in sample Kl 12:21.55+25.5 m probably due to the lower amount of illite/muscovite compared to Kl 10:21.7 m.
- The U and Cs concentrations may thus reflect the relative amounts of Fe-oxyhydroxide and clay mineral phases, respectively.

The chemical composition of the mixed-layer-clay sample (Kl 9:373.9 m) is characterised by very low concentrations of most analysed elements compared to dolerite. Exceptions are Fe which is 2.3 times higher and Cs (and possibly Rb) which are slightly enriched in the mixed-layer clay sample (Tables 5 and 6). The chondrite-normalised REE curve of the clay sample is rather flat with a positive Eu anomaly (Fig. 13) and resembles that of feldspar. Uptake of the large Eu^{2+} ion in feldspar during magmatic processes gives this mineral a characteristic positive Eu-anomaly in chondrite-normalised REE curves (Hendersson, 1984). Weathering of feldspar (in this case plagioclase) might thus have liberated REE, which was then incorporated in the mixed-layer clay (probably after oxidation of Eu^{2+} to Eu^{3+}). This is confirmed by observations in thin sections of selective weathering of plagioclase close to the fracture surface (Fig 14). Alteration of olivine to iddingsite has also been observed. The mixed-layer clay coating was probably formed by in situ weathering and the swelling properties of the clay might give rise to low hydraulic conductivities resulting in limited sorption of elements from the groundwater. Such an interpretation is consistent with the behaviour and chemical compositions of smectite-dominated fracture coatings from dolerite fractures in the Studsvik test site (Landström et al., 1983) and Fjällbacka (Eliasson et al., 1989).

5.2 Hf-normalisation of trace elements in fracture fillings

The net change in concentration of a trace element in a fracture coating relative to that in the original fresh rock provides information on the mobilisation and redistribution of the element in connection with water/rock interaction processes. To correct for the volume change, Ti was used as immobile element in the interpretation of clay alteration effects (cf. section 5.1).

However, Ti was not routinely analysed in the fracture filling samples and therefore had to be replaced with either Zr or Hf, both found to be immobile (Fig. 12). Hf is used in the following calculations of gain and loss of elements owing to the higher accuracy, precision and sensitivity of the analyses of Hf compared to the Zr analyses. The assumption of the immobility of Hf is supported by the fact that most Hf is present in the resistant mineral zircon and that it behaves geochemically more or less like Zr. Furthermore, Hf has been found to be immobile in other studies of weathering (Middelburg et al., 1988). However, one shortcoming is the irregular distribution of Hf in the rock, which makes the use of Hf difficult when investigating fracture minerals formed by selective weathering of e.g. feldspars (cf. Fig 13 and 14).

5.3 Studies of hematite/Fe-oxyhydroxide in fractures at great depth (>500 m vertical depth) and in near-surface fractures (<150 m).

Fracture coatings from a hematite/Fe-oxyhydroxide bearing zone were sampled in the core length interval 613 m to 653 m in sections with different hydraulic conductivities ($<10^{-11}$ to 10^{-6} m/s; Gentzschein, 1986). Hematite, chlorite ± Fe-oxyhydroxide (the latter is lacking in the low-conductivity fractures) and ± calcite dominate the fracture coatings.

The identification of mineral phases using XRD (Table 3) showed that all the samples contained hematite and chlorite (probably of hydrothermal origin). Epidote, which is a hydrothermal mineral usually formed at 300 to 450°C, is found in several samples, which means that this is an old reactivated zone. Of great interest is the presence of goethite in all the samples from below the 620 m level (all samples from the most hydraulically conductive part of the zone), whereas goethite is absent in the two fractures from the sections with low hydraulic conductivity (613.1 m and 617.1 m). In contrast, muscovite/illite is identified only in these two samples. Pyrite was identified together with hematite and Fe-oxyhydroxide in samples Kl 13:624.7 and Kl 13:647.6 m.

Thin sections from the hematite/Fe-oxyhydroxide zone were studied and the results are shown in Table 4, where the relative

ages of the different mineralisations are given. The tectonic history of the area, as described in Table 1 is also verified in the samples studied here. It is suggested that the first and dominant period of hematite formation (which can easily be seen in the thin sections) took place during a period of extensive circulation of hydrothermal and oxidising fluids in the bedrock. This period is probably closely associated with, but post-dates, a period of extensive mylonitisation documented in the area. The possible age of the oxidising event is ≈1400 Ma, as based on e.g. K-Ar ages of a probable metamorphic event in the southeastern Sweden (Magnusson, 1960). Later hydrothermal activity, e.g. in connection with intrusions of the basic dykes (1000-900 Ma), is probably not extensive enough to yield the widespread distribution of the hematite.

In thin section studies of the wall rock close to the fracture edges it can be seen that the frequency of pyrite and magnetite (accessory minerals in the host granite) decreases towards the fractures. In contrast, hematite increases. In two of the thin sections (Kl 13:624.7 and Kl 13:653.3) small grains of pyrite, post-dating the hematite, are visible in the fracture coatings. In sample Kl 13:653.3, magnetite can also be observed at the fracture edge. Based on these observations it is suggested that reducing solutions (probably hydrothermal) have circulated in the fractures after the main oxidising event.

The REEs in samples from fractures with high hydraulic conductivity are strongly fractionated and also correlated with the hydraulic conductivity (Fig.15). The La concentration is as high as 4500 ppm in the most conductive section. Th and U also reach high values (300 ppm and 200 ppm respectively) there. Fracture coatings from sections of low conductivity are low in REEs and have chondrite-normalised REE patterns similar to the granite averages (f and g in Fig. 15). The Th and U contents are also low in these samples, in contrast to the samples from the highly conductive sections.

Figure 16 shows Hf-normalised values of trace elements and illustrates the contrasting chemical compositions of fracture coatings from sections of high and low hydraulic conductivity, respectively. REEs, Th and U are highly enriched while Ba, Rb and Cs are moderately enriched in the fractures from sections with high conductivity (Fe-oxyhydroxide bearing), in contrast to the

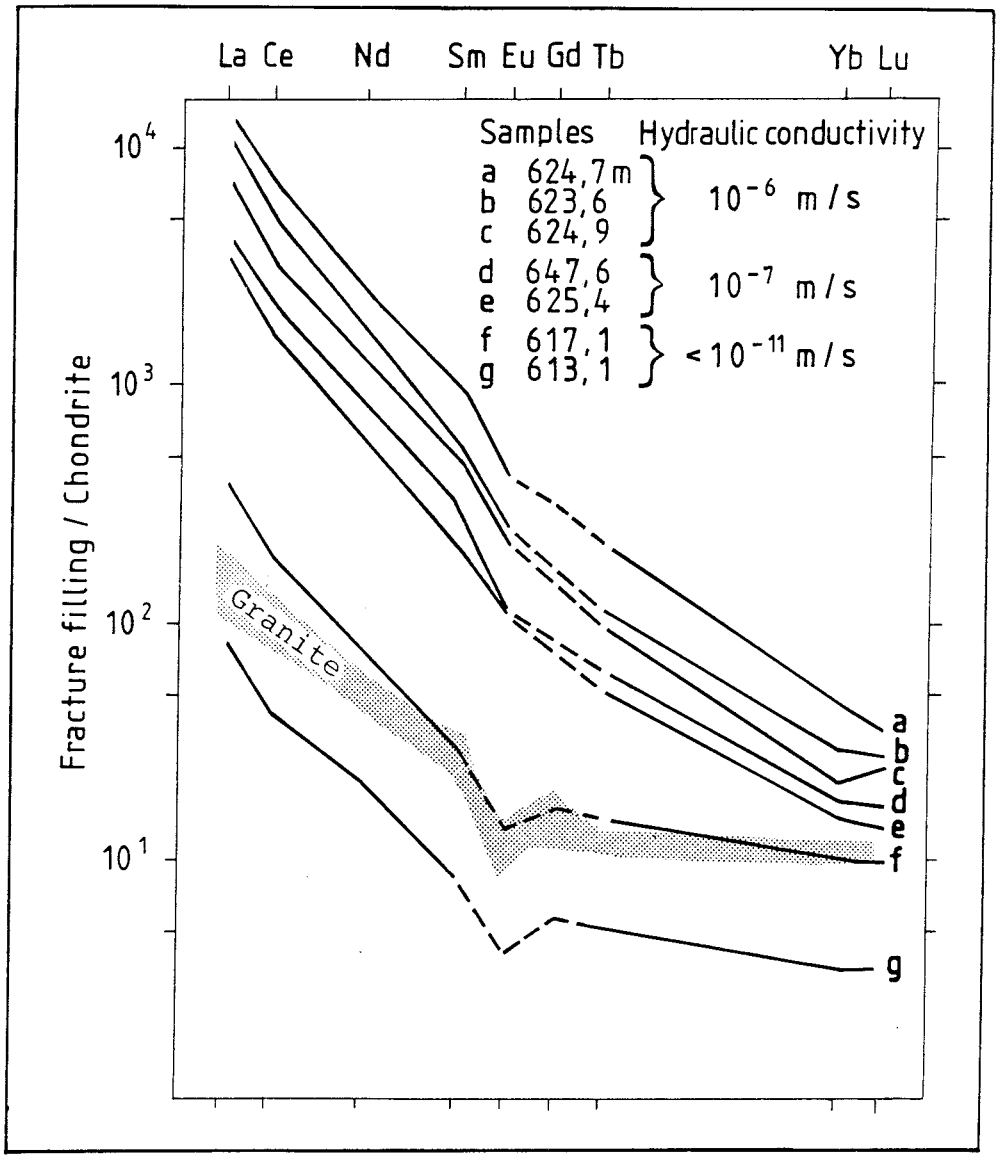

Figure 15 Chondrite-normalised REE pattern of hematite/Fe-oxyhydroxide-bearing fracture coatings from 613.1 m to 649.6 m corelength in drill core Kl 13. Note the different hydraulic conductivities of the fractures.

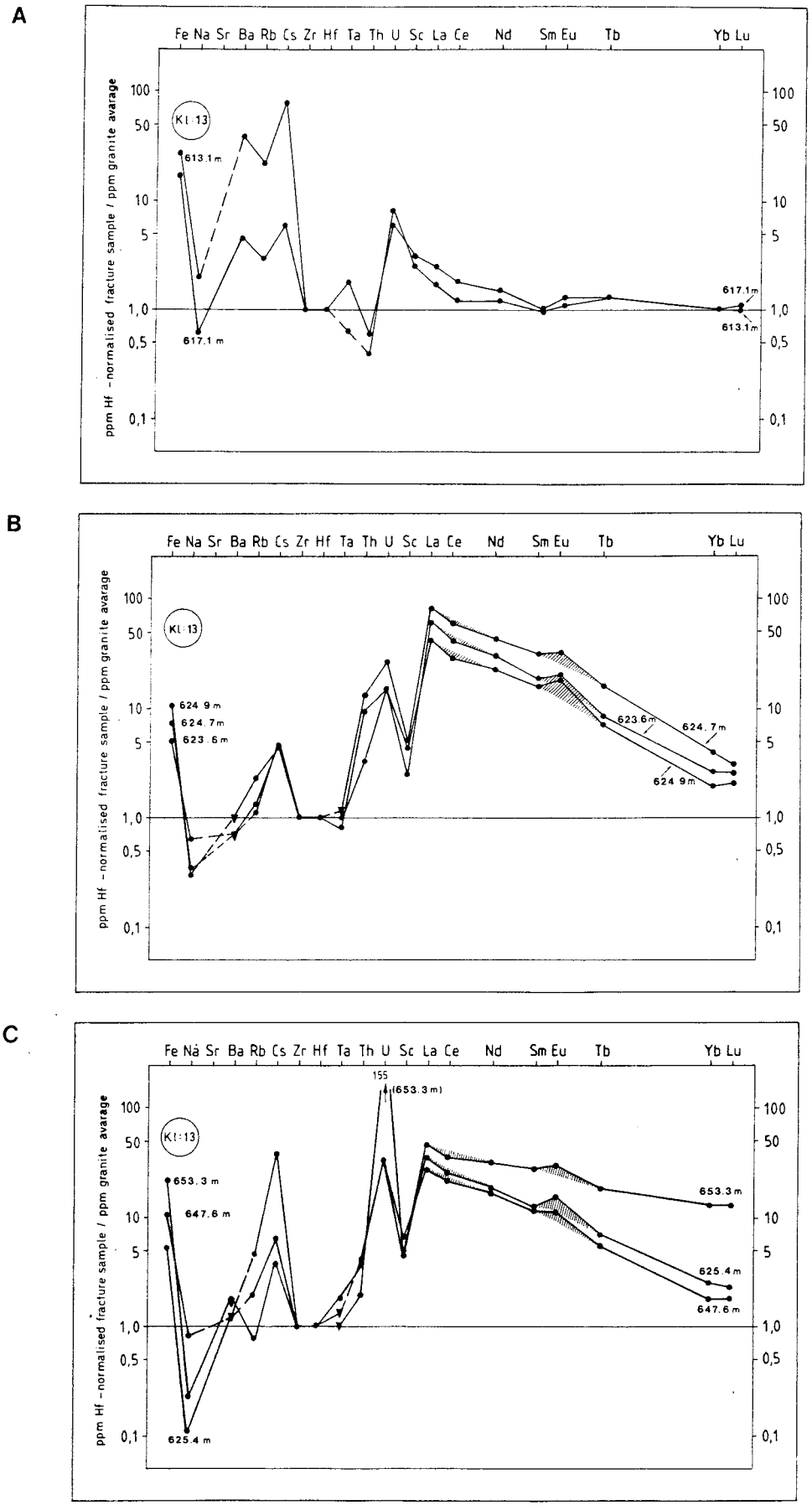

Figure 16 a,b,c, Hf-normalised trace element diagrams from sections with different hydraulic conductivities in the Fe-oxyhydroxide/hematite-coated fracture zone in Kl 13. The plots are grouped according to hydraulic conductivity; a = $<10^{-11}$ m/s, b = 10^{-6} m/s and c = 10^{-7} m/s.

fractures from sections with low hydraulic conductivity (muscovite/illite-bearing) which have higher levels of mobile elements like Na, Ba, Rb and Cs and lower levels of REEs, U, and Th. It is likely that the pronounced enrichment of light REEs, Th and U is associated with the presence of Fe-oxyhydroxide and that the enrichment of elements such as Cs and Rb is correlated to the presence of muscovite/illite, as in Kl 13:613.1 and Kl 13:617.6 m. However, variations in the mineralogy of the fractures from the high and low hydraulic sections cannot alone explain the variation in trace element composition. It is thus probable that redistribution of trace elements due to sorption (U, Th and REE) and leaching (Na, Ba, Rb and Cs) in the more hydraulically conductive parts of the zone is an important process.

Concerning the redox conditions in the zone, it can be concluded that the high U concentration as well as the observations of small pyrite crystals within the the surface layers of the fracture coatings indicate reducing conditions at present. Reducing conditions at these depths is also suggested by analyses performed on groundwater samples from other drillholes in the area. As the Fe-oxyhydroxide in the fractures is likely to be correlated with hematite-coated fractures that are currently hydraulically conductive (Tullborg, 1986), it is probable that water/mineral interaction in an Fe(III)-rich environment causes the formation of Fe-oxyhydroxide at great depths. However, a formation of the Fe-oxyhydroxide as a last phase of a hydrothermal event is another possibilty.

For the purpose of comparison two hematite/Fe-oxyhydroxide-coated, water-conducting fracture at more shallow depth, in a possibly oxidising environment, were analysed (sample Kl 9:28.25 m and Kl 2:122.6 m). The trace element distributions in these samples show patterns similar to those in the hematite/Fe-oxyhydroxide samples at great depth (Fig.17). However, the enrichment of the light REEs is almost one order of magnitude lower in the shallow samples, whereas the levels of heavy REEs are in agreement with the deeper samples in Kl 13 for sample Kl 9:28.25 m but significantly lower for the other shallow sample (Kl 2:122.6 m). The enrichment of U is somewhat lower in the shallow samples compared to the values obtained in the deep fracture zone. This is also true for Th, but the value in sample Kl 2:122.6 m is much lower than in sample Kl 9:28.25.

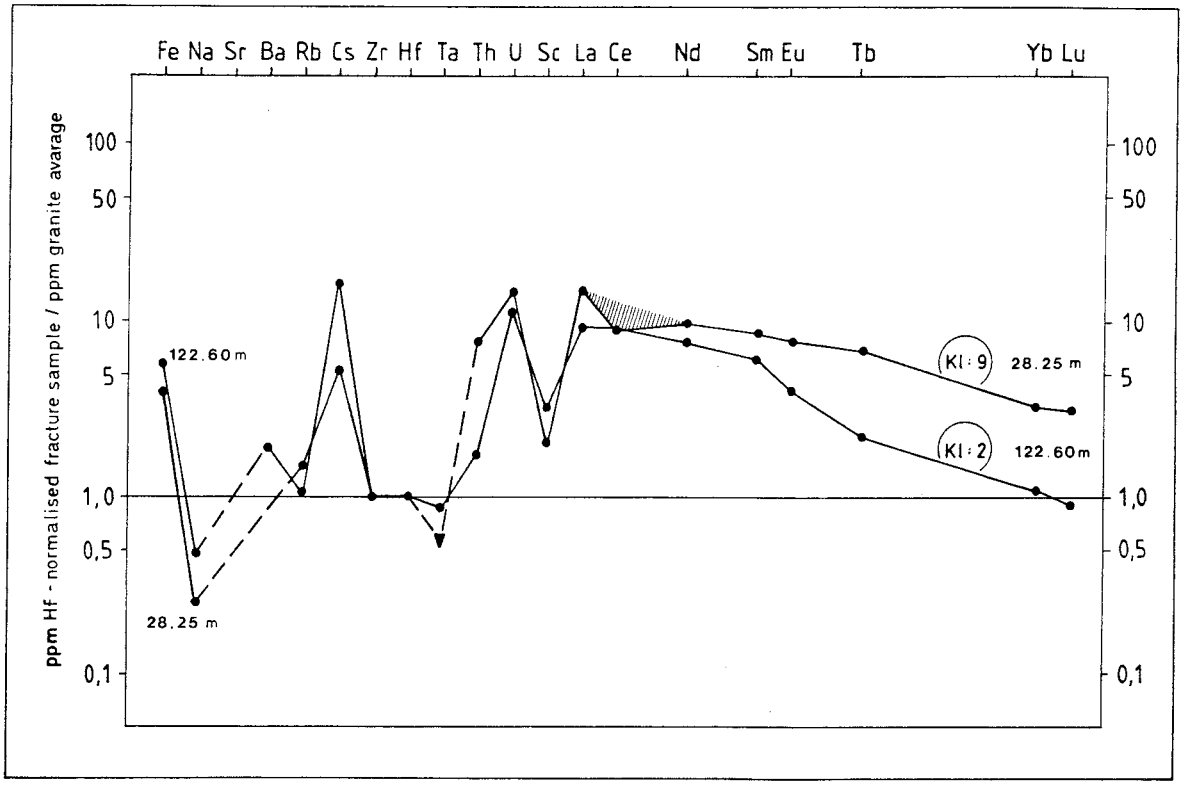

Figure 17 Hf-normalised trace element diagrams for near-surface, Fe-oxyhydroxide/hematite-coated fractures Kl 9:28.25 m and Kl 2:122.60 m.

The same differences in distribution of REEs, U and Th between deep and shallow Fe-oxyhydroxide-coated fractures are observed in Lansjärv (Landström et al. in Bäckblom & Stanfors (Eds.) 1989) There, two hematite/Fe-oxyhydroxide-coated fractures from depths of 76 m and 287 m are compared showing higher values of REEs (especially light REEs, La 41.6 ppm and 188 ppm, respectively), U (6.7 ppm and 31.0 ppm, respectively) and Th (3.7 ppm and 6.0 ppm, respectively) in the deeper fracture sampled (Landström et al., 1989). The uranium series decay data shows marginal disequilibrium for sample 287.7 m, indicating slight water/rock interaction over a long period of time or a very recent phenomenon, while sample 76.2 m clearly shows uranium precipitation, which indicates a transition from oxidising to reducing conditions, possibly still in progress, and points to extensive water/rock interaction, at least within the last 250 000 to 1 million years. This result, combined with the higher U value observed in the fracture filling at great depth (287.7) compared to the near-surface fracture (76.2) further underline the effect of U sorption compared with regular precipitation, mainly occuring in the transition zone between oxidising and reducing conditions.
Rock-normalised concentrations of the elements Fe, Sc, Th, U, La, Yb, Na and Cs for the fracture coating (A) and the wall rock samples (B and C) are compared for the two levels in KLj 1, Lansjärv (Fig. 18). Most of the samples show a slight increase from the C to B samples which may be due to circulation of hydrothermal fluids in the fracture, causing an enrichment of these elements in the adjacent wall rock. Striking differences between the two borehole levels can, however be seen for the U, Cs, Na and REEs (especially the light REEs) concentrations in the fracture coating samples compared to those in the wall rock samples. In sample 76.2 m a decrease of these elements is recorded in the fracture sample. This may be indicative of a low temperature redistribution of these elements described as leaching in the near-surface region, and a sorption of, in particular, light REEs and U onto hematite/Fe-oxyhydroxide phases superimposed on the original hydrothermal enrichment of the trace elements close to the fracture.

In conclusion, results from both areas (Lansjärv and Klipperås) indicate that leaching of REEs, especially light REEs, occurs in the upper zone, probably facilitated by oxidising conditions and

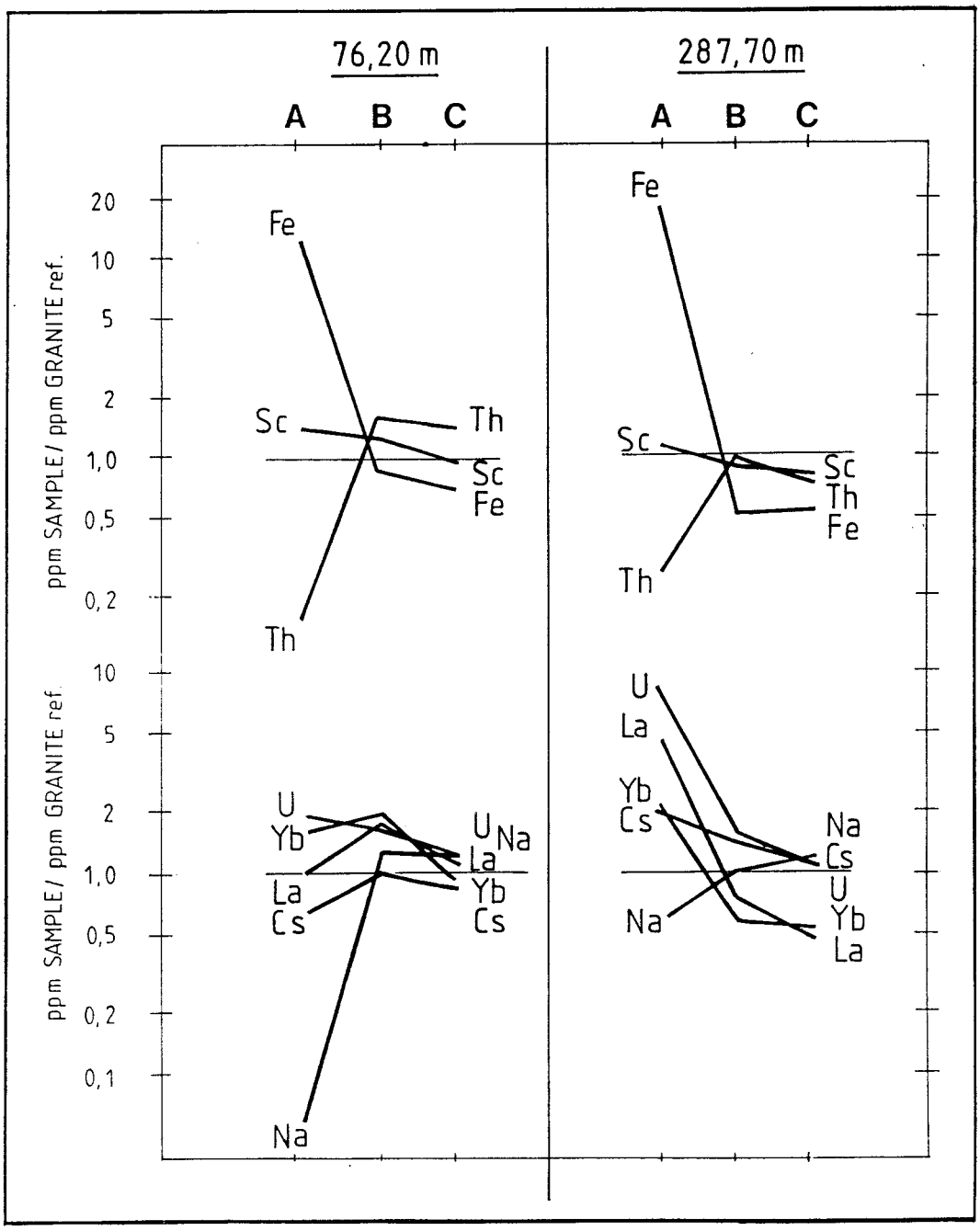

Figure 18. Trace element distribution in fracture filling (A) and in wall rock (B and C) in relation to the granite average for sample 76.6 m and 287.7 m in drill core KLJ 01 in Lansjärv (Landström et al.,1989). A is fracture fillings, B and C wall rock samples. The length of the profile A, B, C is 3-4 cm.

CO_2-rich water causing breakdown of minerals (saturation indices are low for most of the minerals present). Futhermore, a high HCO_3 content in the water (usually found at shallow depth) results in a relatively higher mobility of the REEs due to complexation. All this is in contrast to the situation at great depth where sorption and coprecipitation are favoured by the chemical conditions, e.g. the relatively lower HCO_3 content of the groundwater at great depth. However, HREEs tend to form stronger carbonate complexis then the LREEs i.e. a higher mobility of the HREEs whould be expected in contrast to the observed higher mobility of the LREEs. This underlines the selective leaching/sorption of LREEs in the Fe-oxyhydroxide/hematite coatings.

Concerning U, the uranium decay series isotopes suggest recent deposition of U (cf. Lansjärv 76 m and Klipperås Kl 7:125 m section 5.4), but the total amount of U is still lower in these samples than in comparable samples at great depth. The more pronounced enrichment of U, Th and REEs undoubtedly found at great depth may reflect the potential of sorption processes.

5.4 A near-surface zone (Zone 4)

Zone 4, which strikes NE and dips 65° to SE (Fig. 3), consists of completely crushed material with angular shaped grains of size 0.1 to 2 mm strongly indicating in situ brecciation and formation. The mineral composition of the fragments shows that metabasite and granite, together with porphyry, are all present. Some pieces of greenstone show a thin rim of clay minerals. There are also pieces of old fracture fillings included in the crushed material, indicating that this is an old reactivated fracture zone. Some of the grains are cemented together with Fe-oxyhydroxide (Fig. 19).

This zone has received special attention in previous studies as a "late", possibly neotectonic, reactivation is suggested for the zone due to e.g. the sparse sealing and alteration of the angular grains in the zone (Olkiewicz and Stejskal, 1986). The investigations carried out so far (Tullborg 1986a, 1986b, Smellie et al., in manuscript) are briefly summarised in the following:

The distribution of calcite in the fractures (Fig. 6) shows an absence or a very low frequency of calcite-coated fractures down to and within the zone, but below the zone a dramatic frequency

increase is observed. It is therefore probable that this highly conductive zone serves as a barrier, preventing downward penetration of recharge groundwaters. Two samples containing calcite were analysed for $\delta^{18}O/\delta^{13}C$ and yielded values of -4.1/-17.7 o/oo (sample A, Fe-oxyhydroxide- enriched) and -9.0/-12.4 o/oo (sample B, "matrix"). The results are given in per mille and related to PDB. The quite different isotopic signature of the two samples indicates that calcite of different generations occurs within the crushed material and potentially in the cement. Sample B is likely to be close to the isotopic values expected for calcite precipitated under present conditions in the area.

One composite sample from zone 4 containing both single and cemented grains was analysed for ^{14}C (Possnert and Tullborg, 1989) and yielded results of 72.5 pmC (percent modern carbon). Because of the very low carbonate content of the sample, this result can only tentatively suggest a rapid recharge of ^{14}C-rich water to this depth (c. 100 m).

Within a project financed by SKI (Swedish Nuclear Power Inspectorate) concerning dating of neotectonic movements, two samples from the crush zone have been analysed for uranium decay series isotopes (Fig. 20) (Smellie et al, in manuscript). Both samples exhibit disequilibrium, which indicates that low temperature rock/water interaction processes have been active during the last million years or so, and are still active. Sample A, consisting of Fe-cemented grains, which plots well within the uranium deposition field (Fig. 20), indicates a continous process of uranium deposition, suggesting that uranium has been sorbed onto the Fe-oxyhydroxide cement. It is also suggested that the depth of the sampled zone (c. 100 m) corresponds approximately to the depth where oxidising conditions change into reducing. This is supported by sample B (single grains) which also plots within the field of uranium deposition (Fig. 20), but within the sector indicating that the uranium accumulation process has been less continuous and more discrete in nature.

In conclusion, the near-surface crush zone (Kl 7:125 m) is assumed to be a reactivated fracture zone once initiated along dykes of metabasites and porphyry. It has not been possible to establish the age of the reactivation, but a "recent" (neotectonic) origin is not contradicted by the available results. Furthermore, the results suggest an intense water circulation in

the zone.

Two samples were analysed for trace elements; one sample (B) contained only single sharp-angled grains, while the other sample (A) contained only grains cemented together with what seems to be Fe-oxyhydroxide. The results are presented in Table 6 and in Figure 21. If it is assumed that the overall composition of the grains approximates 60% greenstone, 20% porphyry and granite and 20% quartz and old fracture fillings, a composition roughly in accordance with optical microscopy observations, then Zr, Hf, Ta, Th, Sc and REEs are present in expected concentrations (i.e. these elements are not significantly mobilised or enriched in the crushed material). In contrast, Rb, Ba, Cs, Zn, and Sb are all present in higher concentrations (in both samples) than is expected from the rock analyses in Table 5. This means that these elements have been supplied by the groundwater, e.g sorbed on recently formed clay minerals, and/or that they are present in old fracture fillings included in the crushed material. The slightly higher values of these elements in the Fe-oxyhydroxide sample may be due to coprecipitation of these elements in the oxyhydroxide and/or to a possibly higher amount of clay minerals in this sample. Cr and Co may have been supplied by the groundwater, but there is also a possibility of contamination.

Uranium is the only element that is clearly correlated to the Fe-oxyhydroxide. However, an excess of uranium, compared to the rock samples, is also observed in sample B containing only single grains. This means that U, like Cs, Rb, Ba, Zn and Sb, may have been sorbed on the thin rims of alteration products (probably clay minerals) surrounding the greenstone grains especially.

Compared to other hydraulically conductive fractures containing hematite/Fe-oxyhydroxide at great depth, uranium enrichment is lower and thorium and REEs are not enriched compared to the host rock in this "near surface" zone (cf. section 5.3). However, the uranium series decay data for sample Kl7:125 m points to precipitation of uranium as resulting from changes from an oxidising to a reducing environment. This agrees with the results discussed in section 5.3.

Figure 19. Photo of thin section showing single grains cemented together by Fe-oxyhydroxide. To the right a grain of basite surrounded by a thin rim of clay minerals (Kl 7:125m).

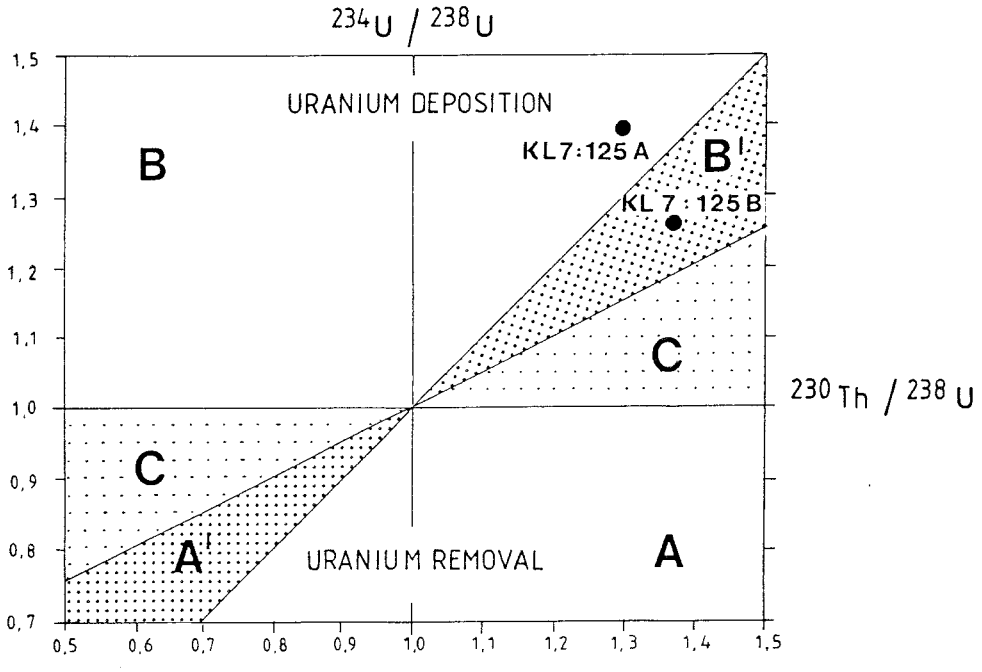

Figure 20. Thiels plot of uranium series data for Kl 7:125 m A (containing Fe-oxyhydroxide cement) and Kl 7:125 m B (containing only single grains). A^1 and B^1 = interval forbidden for continous single processes. C^1 = interval forbidden for any single process.

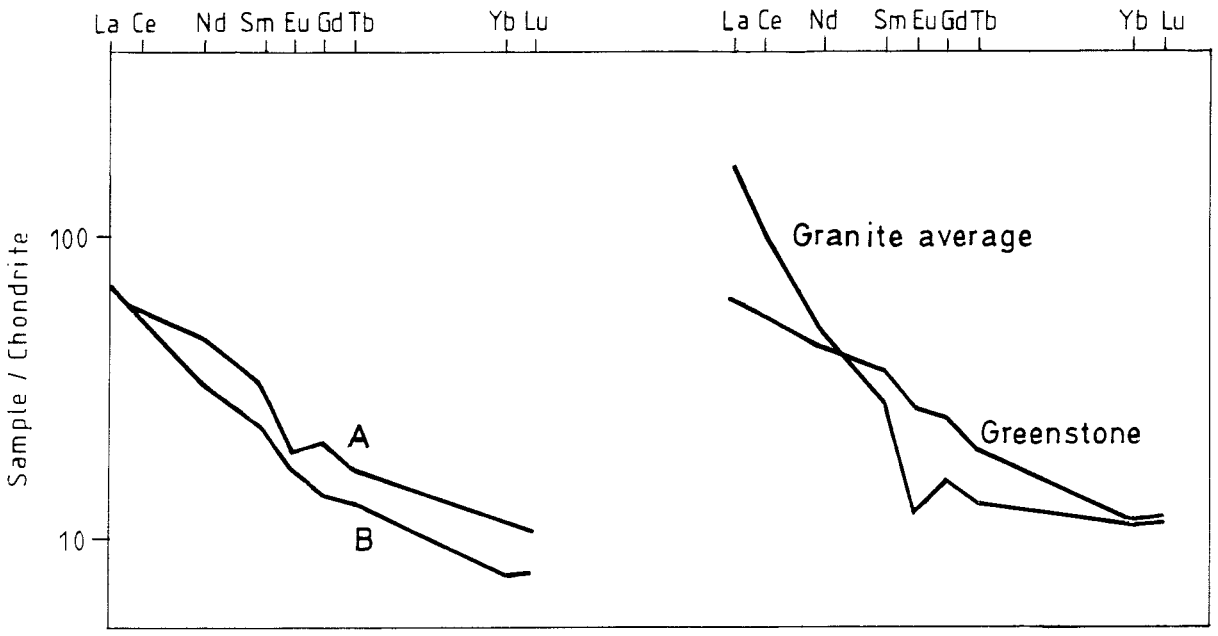

Figure 21. Chondrite-normalised REE patterns for samples Kl 7:125 m A and B and for comparision the REE curves for granite and greenstone.

5.5 Ce and Eu anomalies

In contrast to other trivalent REEs, Ce and Eu can occur in other oxidation states; in nature Ce^{3+} can be oxidized to Ce^{4+} and Eu^{3+} reduced to Eu^{2+}. The different chemical properties of Ce^{4+} and Eu^{2+} compared with the trivalent REEs result in a marked divergence in their geochemical behaviour, which can give rise to positive and negative anomalies in chondrite- or rock-normalised REE patterns (Fig. 22).

The redox sensitivity of Ce and Eu can be utilized for estimations of redox conditions in the past and present. The oxygen fugacity prevailing during mineral formation has thus been determined from Eu^{2+}/Eu^{3+} ratios in minerals (Hendersson, 1984; Drake & Weill, 1975). Concerning Ce, it is known that Ce^{3+} in carbonate media is easily oxidised to Ce^{4+} by air, i.e surface conditions (Ferri et al., 1983). Another possible application, of interest in studies and predictions of actinide migration would be the use of Ce and Eu anomalies as natural "tracers" for REE migration paths. This is based on identification of the mobilisation ("source") and sorption ("sink") sites and additional measurements of the water REE pattern. An example of this approach is given in a study of trace elements in the Lansjärv neotectonic zone in northern Sweden (Landström et al., 1989) and is briefly recapitulated below.

At Lansjärv both positive and negative Ce anomalies were found in the fracture coatings as well as in the adjacent, slightly altered wall rock. The anomalies are absent in the fresh granite and can thus be concluded to have formed through post-emplacement water/rock interactions. As seen in Figure 22, positive Ce anomalies occur only in fractures and adjacent wall rock samples in the upper part of the drill core whereas the more pronounced negative Ce anomalies are found deeper down. These observations are explained as follows:

Oxidation of Ce^{3+} to less mobile Ce^{4+} present in the fracture mineral coating or in the adjacent wall rock, together with mobilisation and removal of the trivalent REEs have caused the positive Ce anomalies in the mineral phases in the upper part of the drillcore (Fig. 22) while the transporting medium (i.e. groundwater or hydrothermal fluids) is depleted in Ce compared to the other REEs. Mineral/water interactions, e.g. sorption and/or

mineral precipitation involving Ce-depleted water, give rise to the negative Ce anomalies found in minerals along the water conducting fractures at great depths (Fig. 22). The oxidation may in this case be of hydrothermal origin (coeval with extensive formations of hematite/Fe-oxyhydroxide) and the redistribution of the REEs (which produces the positive and negative Ce anomalies) may have been mediated by circulating hydrothermal fluids or subsequently by low temperature groundwater.

Pronounced Ce anomalies, like those found in the Lansjärv samples, were not found in the fracture coatings from Klipperås. Small negative Ce anomalies are indicated in the REE patterns of the hematite/Fe-oxyhydroxide zone in Kl 13 (624-653 m, figs. 15 and 16). Sample Kl 9:28.25 m also shows a negative Ce anomaly compared to the granite average (Fig. 17). As no systematic study of e.g. altered wall rocks in the upper oxidising zone has been made, one cannot exclude the possibility of positive Ce anomalies, such as is the case at Lansjärv.

Negative Ce anomalies, exemplified in Figure 28, were also found in peat and clay samples from the bottom layer of a peat bog situated above fracture zone 13 in the western part of the Klipperås area (Fig. 3) (Landström & Sundblad, in prep). A study of radionuclides in the U and Th decay series indicated an inflow to the bog of groundwater from the fracture zone below (Landström & Sundblad, 1986). The negative Ce anomaly in the peat may thus be the result of REE migration from e.g. an oxidised upper horizon in the bedrock (such as in the Lansjärv case) via fractures to the bog. Findings of positive Ce anomalies in Mn-rich bog ores point, however, to an alternative or complementary process: Oxidation of Ce^{3+} to Ce^{4+} followed by coprecipitation of Ce^{4+} with Fe- and Mn-oxyhydroxide in the initial lake stage. Precipitation/sorption of trivalent REE from the Ce-depleted lake water will then cause the negative Ce anomalies found in the bottom clay sediments and peat layers (Landström & Sundblad, in prep.).

Granite-normalised REE curves of fracture coatings, especially those at great depths, show positive Eu anomalies (Figs. 15 and 16). One interpretation could be the following: In feldspars Eu is usually enriched in divalent form relative to the other REEs, e.g. positive Eu anomalies are typical of feldspars. Oxidation of Eu^{2+} to Eu^{3+} in connection with selective weathering of feldspars (cf. section 5.1 and Figs. 13 and 14) followed by mobilisation of REEs

whould thus result in Eu-rich groundwater/hydrothermal fluids. Subsequent precipitation whould then produce positive Eu-anomalies in granite-normalised REE patterns of the fracture precipitates.

Identifying sources (zones where oxidation of Ce and Eu have occurred in the past or present) and sinks (zones of precipitation/sorption of REEs from water or hydrothermal fluids which are anomalous in Eu or Ce), combined with a knowledge of the local hydrology, could thus yield site-specific information regarding possible migration paths for REEs and actinides.

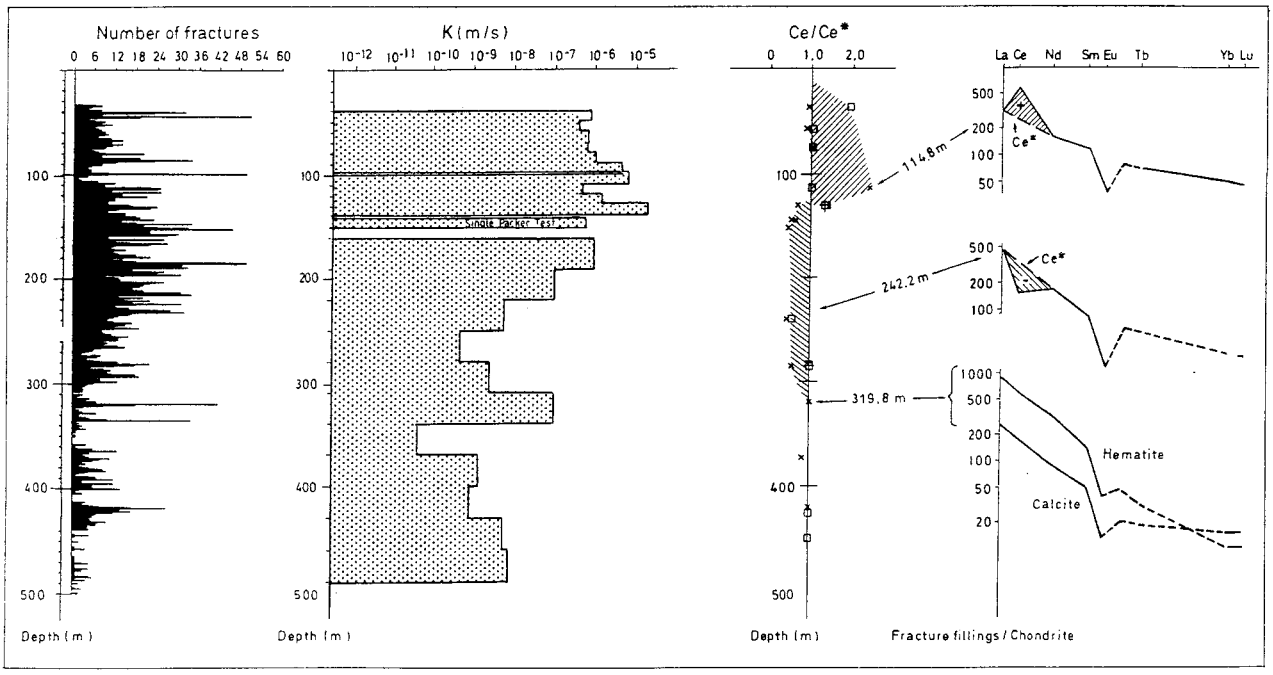

Figure 22. Compilation of hydraulic conductivity, fracture frequency and Ce/Ce* versus depth for drill core KLJ 01 from Lansjärv (Landström et el., 1989)

5.6 Distribution coefficients for fracture mineral/groundwater phases ("in situ K_d's")

The mass distribution coefficient, K_d, an important parameter in modelling radionuclide migration in crystalline rocks, is usually determined in laboratory experiments on rock and mineral samples. However, in such experiments, it is difficult to completely simulate the complexity of processes, reacting minerals and geochemical parameters involved in radionuclide transport in fractures during long periods of time. It is therefore important to verify the validity of the laboratory data by e.g. measurements of current chemical equilibria between groundwater and fracture minerals. As a first approach in this direction, we have estimated mass distribution coefficients (here called "in situ" in contrast to laboratory-determined) from analyses of fracture coatings and groundwater sampled from the same fracture zone.

The three representative groundwater samples (i.e. groundwater not contaminated with water from other sources) Kl 1:406 m, Kl 2:326 m and Kl 9:696 m (Smellie et al., 1987) and corresponding fracture fillings were chosen for the K_d study. Trace and major element compositions are shown in Tables 7a and 7b (groundwaters) and Table 6 (fracture fillings) and mineral compositions are given in Table 3.

As far as the groundwater chemistry is concerned, two groundwater types were identified according to Smellie et al. (1987): groundwaters of near-surface origin (Ca-HCO_3 type; Kl 2:329 m and Kl 9:696 m) and of intermediate origin (characterized by decreased contents of Ca, Mg and HCO_3 in comparison with the near-surface waters; Kl 1:406-564 m) see Figure 23. No saline waters were detected in the area. Reducing conditions as well as a stable pH between 7.6 and 8.3 (see Table 7b) characterised all three samples.

Chemical equilibrium modelling showed that the sampled groundwaters are nearly saturated with respect to calcite and other carbonate minerals and that Fe^{3+} and Al^{3+} appear to be saturated with their hydroxides (Smellie et al., 1987). Analyses of fillings from the corresponding fracture zones confirmed this: the carbonates; calcite and siderite as well as goethite (Fe-oxyhydroxide) and gibbsite (Al-hydroxide) were identified (Tullborg, 1986; Smellie et al., 1987 and Table 3). Other identified Al-minerals

are e.g. chlorite (14-Å chlorite, probably of hydrothermal origin) and muscovite/illite. Kaolinite was also found (Kl 2:329.65 m) which is surprising as the formation of this mineral is favoured by near-surface conditions. The observations described above support a conception of fractures in which mineral formation and mineral/water reactions are now occuring but they also illustrate the complex history of fractures (and their coatings) which at present are water-conducting.

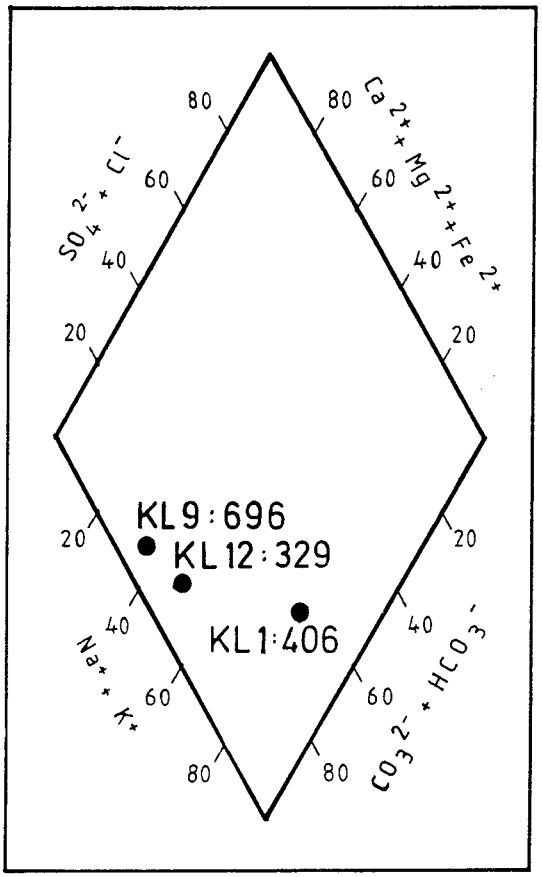

Figure 23. Piper plot of the three representative groundwater samples from Klipperås.

The fracture fillings from Kl 1:438.8 m, Kl 1:440.3 m and Kl 2:329.65 m all contained muscovite/illite, quartz and K-feldspar. In addition, calcite and hematite were found in sample Kl 1:440.3 m and chlorite and calcite in sample Kl 2:329.65 m. Sample Kl 9:696.35 m differs from the others in that it contained epidote as the dominant fracture filling as well as goethite, quartz, gibbsite and siderite. Most of the fracture coatings were stained red possibly due to the presence of very small amounts of Fe-oxyhydroxide or hematite (not detecTable by XRD). We believe that in these samples the most active fracture minerals in the sorption processes are: illite/muscovite, carbonates, Fe-oxyhydroxide/-hematite and possibly chlorite and epidote.

Two sets of K_d's (K_d = conc. in fracture filling/conc. in groundwater) are presented in Table 8, "whole sample" and "Hf-corrected" K_d's, respectively. The "whole sample" K_d is based on the total concentration in the fracture filling sample. These concentration values may include fractions of elements which originate from the adjacent ("parent") rock and are found in e.g. remnants of resistant minerals from alteration processes and/or in rock fragments released in the sampling procedure. This contribution has been corrected for by assuming an element to be immobile and its concentration in the fracture filling to be representative of the rock-derived fractions. In this case Hf has been used, for reasons given in section 5.2. The correction formula is given in Table 8.

The Hf-corrected K_d's (Table 8) are thus based on the fraction of the analysed element concentration which has been supplied from the fluid phase (i.e. the excess part for elements with ratios >1 in the Hf-normalised diagram in Fig. 24). The difference between the two sets of K_d's ("whole sample" and "Hf-corrected") is illustrated by e.g. the K_d's estimated for the muscovite/illite sample, Kl 10:21.70 m. There, the "whole sample" K_d for Th is >2100 m^3/kg while the Hf correction shows that Th probably has not been added to the clay sample and the value of the "whole sample" K_d is thus meaningless. We consider the Hf-corrected K_d values to be more realistic and they are also in better agreement with the laboratory-based K_d values, which are calculated from the amount of radionuclides sorbed from a water phase on a solid rock or mineral phase.

K_d values for the illite/muscovite (Kl 10:21.7 m) and Fe-

Table 8 Distribution coefficients (in situ K_d's)

Element	Measured K_d's[1] m^3/kg						Estimated K_d's[2] m^3/kg			Clay/pore water[5]				Fracture illite/groundwater[6]		
	Kl 1: 406 m		Kl 2: 326 m		Kl 9: 696 m		Kl 10: 21.7 m		Kl 13: 624.7 m	Whole sample		Separated phases		whole sample	amorph Fe	ion exchange
	whole sample[3]	Hf-corr.[4]	whole sample	Hf-corr.	whole sample	Hf-corr.	whole sample	Hf-corr.	Hf-corr.							
Rb	160	28	66	46	22	-	86	27	42							
Sr	1	-	2	1.7	4	3.3			-							
Cs	110	70	6030	6000	19	10	307	292	26							
Ba	30	-	10	6.7	5	-	16	2	-							
Co	300	-	210	190	240	77	140	34	-							
Zn	7	-	42	38			43	31	-							
Th	>2700	>1500	> 700		>2800	>1300	>2100	—	10000	57.8	145	276	1730	250	9.8	0.077
U	97	89	10	8.6	85	71	13	9	63	2.0	1.7	23.2	13.8	1.3	0.49	0.012
Sc	4450	550	2000	1200	7600	6000	3200	1100	4600							
La	>5800	>4800	5000	4600	>11000	>11000	1200	360	40000							
Ce			2900	2600	6800	6300	1060	390	23000							
Sm			500	400												
Eu	1060	-	900	650	1400	1100			10000							
Tb	> 73	> 20	180	130												
Yb	>150	> 50	80	20	> 370	> 160										
Lu	870	400	120	30	250	120	340	120	270							

1) From fracture fillings/groundwater pairs
2) Estimated using average values of the three groundwaters, Table 7a
3) based on the total concentration in the fracture filling sample
4) Based on concentrations, corrected for rock-derived element fractions: $C_{corr.} = C_s - \frac{Hf_s}{Hf_{gr}} \cdot C_{gr}$, where

C_s = measured concentration, sample Hf_s = Conc. Hf, sample
C_{gr} " " , granite average Hf_{gr} = " Hf, granite average

5 From Ivanovich et al., 1988
6 From Dearlove et al., 1989

($K_d = C_{corr\ in\ fracture\ coating} / C_{groundwater}$)

A

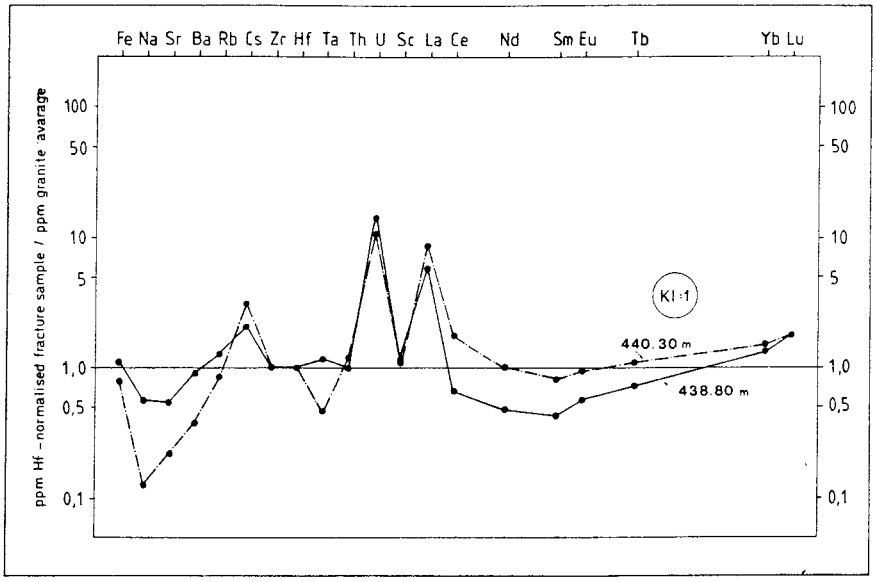

B

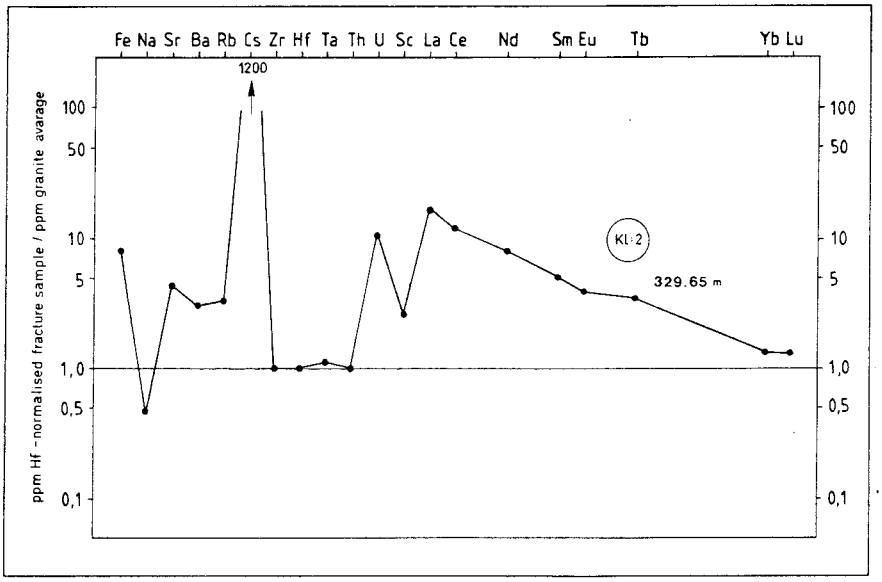

C

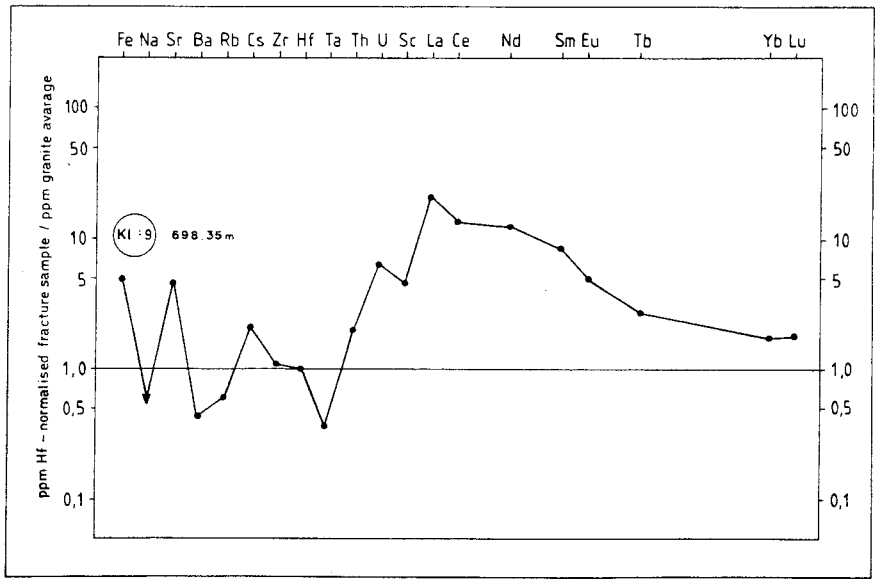

Figure 24. Hf-normalised trace element diagram for samples Kl 1: 438.8 m and 440.3 m (a), Kl 2:329.65 m (b) and Kl 9:698.35 m (c).

oxyhydroxide/hematite (Kl 13:624.7 m) samples were estimated from average values for the three analysed groundwaters and are presented in Table 8. However, the groundwater percolating in the clay-altered fracture at c. 20 m depth probably has a different composition from the analysed groundwater from depths exceeding 300 m and consequently the K_d's for the illite/muscovite sample should be regarded as merely rough estimates. The values are nevertheless, of the same order of magnitude as the "in situ" K_d's calculated for the fracture filling/groundwater pairs except for the REEs, which are about one order of magnitude lower in the clay sample. The average groundwater values are probably representative of the water flowing in the Fe-oxyhydroxide/hematite-coated fractures at great depths. Note the high K_d values for the light REE in this zone.

In the following the "in situ" K_d's are discussed for some groups of elements. Unless otherwise specified, the Hf-corrected K_d's for the fracture filling/groundwater pairs are referred to in the discussions.

U and Th

The distribution coefficients vary between 9 and 89 m^3/kg for U and exceed 700 m^3/kg for Th (Table 8). The same table presents results from similar measurements of in situ K_d's for clay/pore water pairs (Ivanowich et al., 1988) and fracture filling (illite)/groundwater pairs (Dearlove et al.,1989). Two sets of K_d's were measured in each of the studies referred to: whole rock and separated phases.

Concerning the study presented by Ivanovich et al. (1988), the K_d's of the whole clay/porewater pairs are slightly lower than the values recorded for the Klipperås samples, but the K_d's of the separated phases (classified as: ion exchangeable, adsorbed ions, amorphous Fe-oxyhydroxide and carbonate) are of the same order of magnitude as the Klipperås values. The whole illite/groundwater K_d's (Dearlove et al., 1989), which probably correspond most closely to the Klipperås fracture filling/groundwater pairs, are about one order of magnitude lower than the values for the Klipperås samples and the K_d's of the separated phases (ion exchangeable and amorphous Fe) are even lower.

The differences between the two sets of K_d's are explained as due to different water flow rates and water/rock ratios, respectively (both being lower in the clay/pore water pairs which show the highest K_d's) (Dearlove et al., 1989). This doesn't apply, however, to the high-conductivity fracture zone at Kl 13:624 m for which the K_d's of Th and U are rather high (Table 8).

The importance of measuring the K_d's of separated phases is stressed by Dearlove et al. (1989), and they claim that these K_d's ("effective K_d's") should be a more realistic measure of the water/rock interaction. The amorphous Fe phase was found to be the most efficient one in retarding U and Th (Dearlove et al.,1989). Although not analysed as separate phases we believe that in Klipperås as well, Fe-oxyhydroxide and hematite play dominant roles in retarding not only U and Th but also the LREEs (cf. Table 8).

REEs

Compared to the granite average, the REE patterns of the fracture filling in Kl 2:329.65 m are strongly enriched and the groundwater depleted in the light REEs (Fig. 25).
This results in La K_d values being one or two orders of magnitude larger than the Lu K_d values. The smooth K_d/ion radius curve (Fig. 26) points to a dependence on the ion size for the sorption process in these mineral phases. The REE pattern of Kl 9:698.35 m is rather similar to that of Kl 2:329.65 m, while those of Kl 1:438.8 and Kl 1:440.3 m differ markedly (Fig. 27). Whether this is related to the two groundwater types (cf. Fig. 23) or not, is not clear.

The low precision of the groundwater REE analysis makes any discussion of changes in the groundwater REE pattern due to selective uptake on fracture fillings uncertain (e.g. that selective sorption of light REEs on the fracture fillings may contribute to the lower light REE/heavy REE ratio of the groundwaters as compared to the granite average (Fig. 25). It is, however, interesting that the close similarity between the REE patterns of peat from a bog in the study site and the granite average (Fig. 28) indirectly suggests a granitic REE signature of surface and near-surface waters, since the majority (> 95%) of the

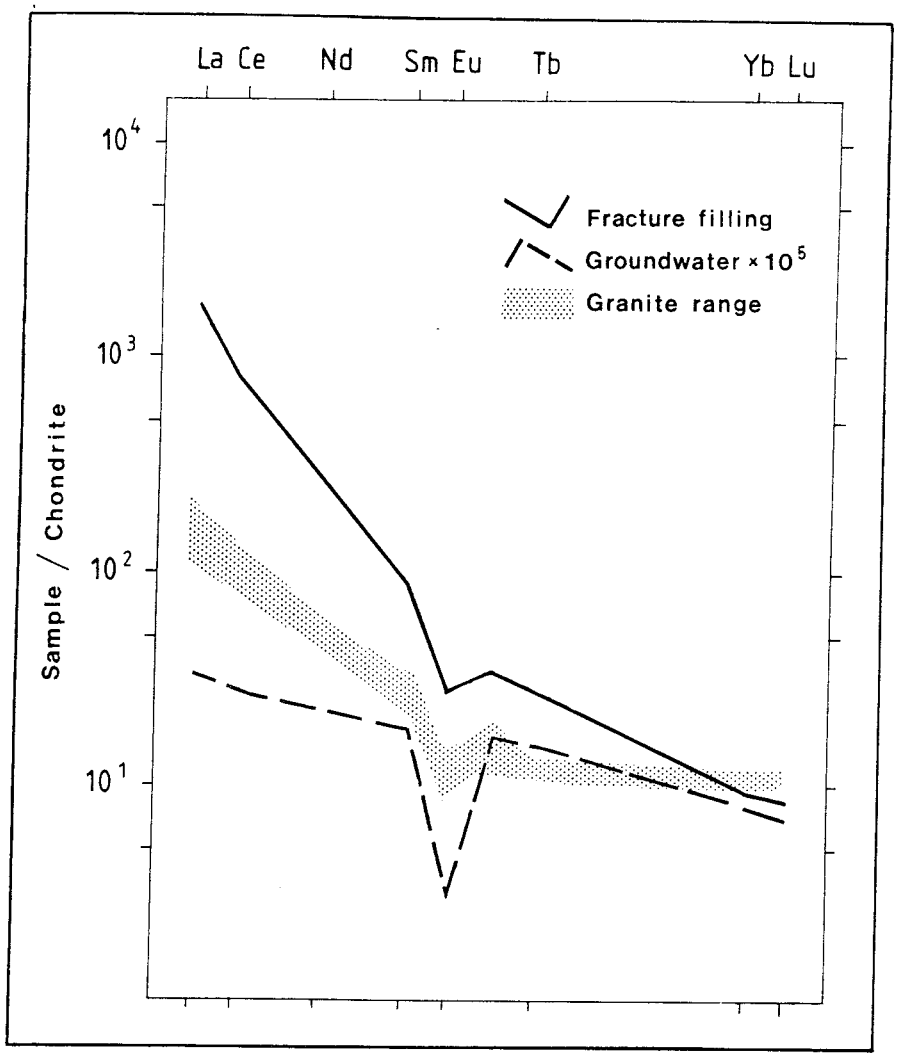

Figure 25. Chondrite-normalised REE patterns of fracture filling, corresponding groundwater and host granite (Kl 2:329 m).

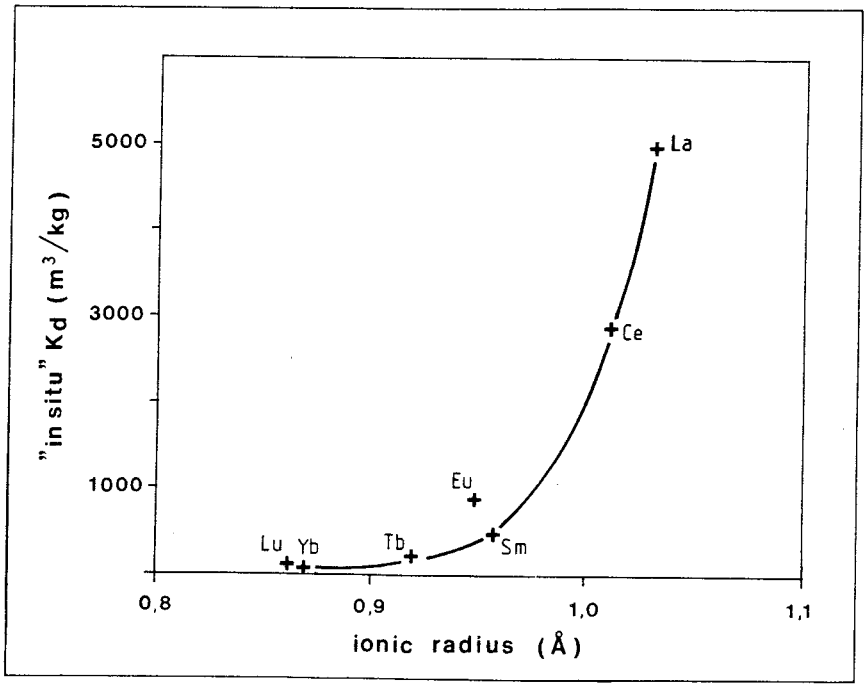

Figure 26. Variation of distribution coefficients ("in situ" K_d's) with ionic radius (Å) for REEs (Kl 2:329.65 m).

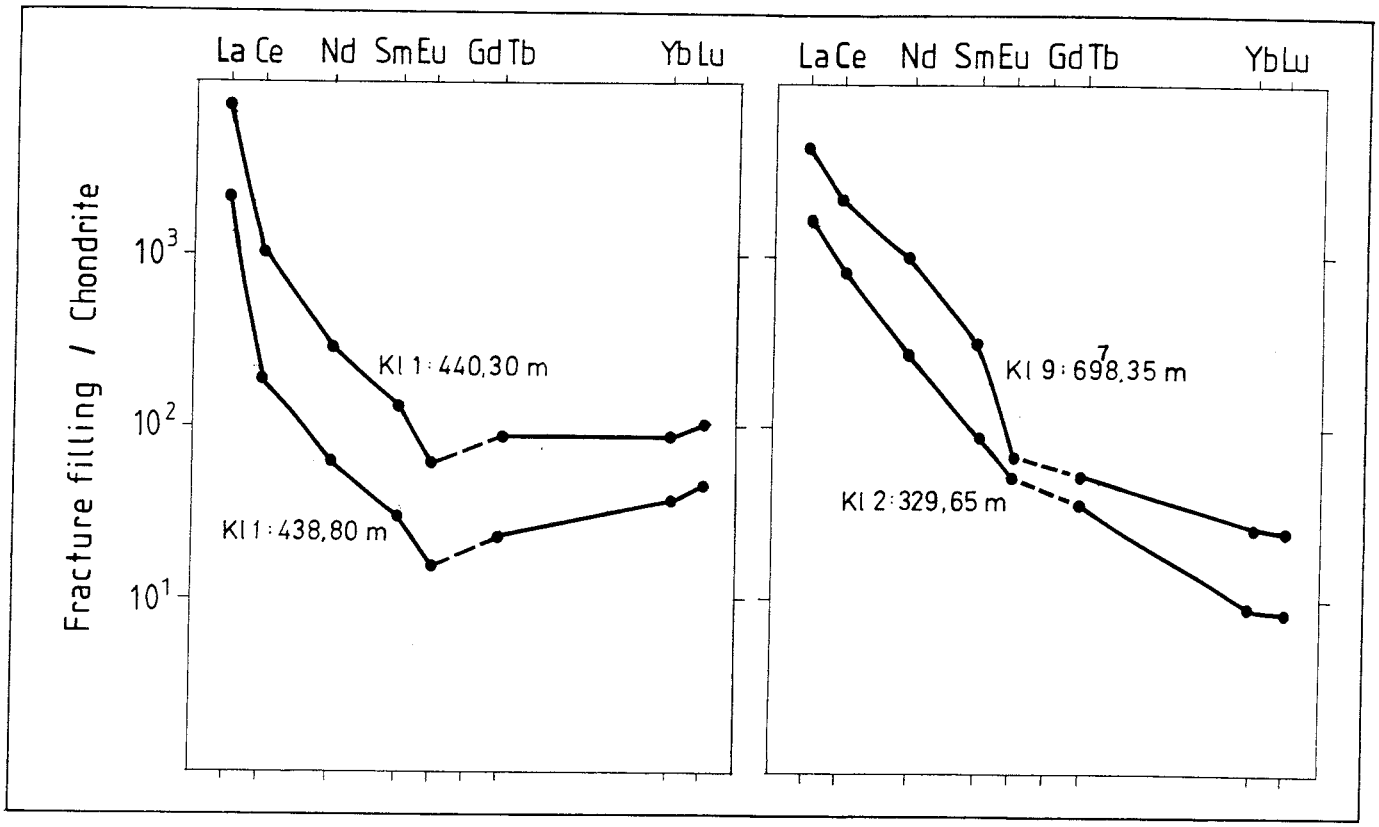

Figure 27. Chondrite-normalised REE patterns for fracture coatings Kl 1:438.80 m, Kl 1:440.30 m, Kl 2:329.65 and Kl 9:698.35 m.

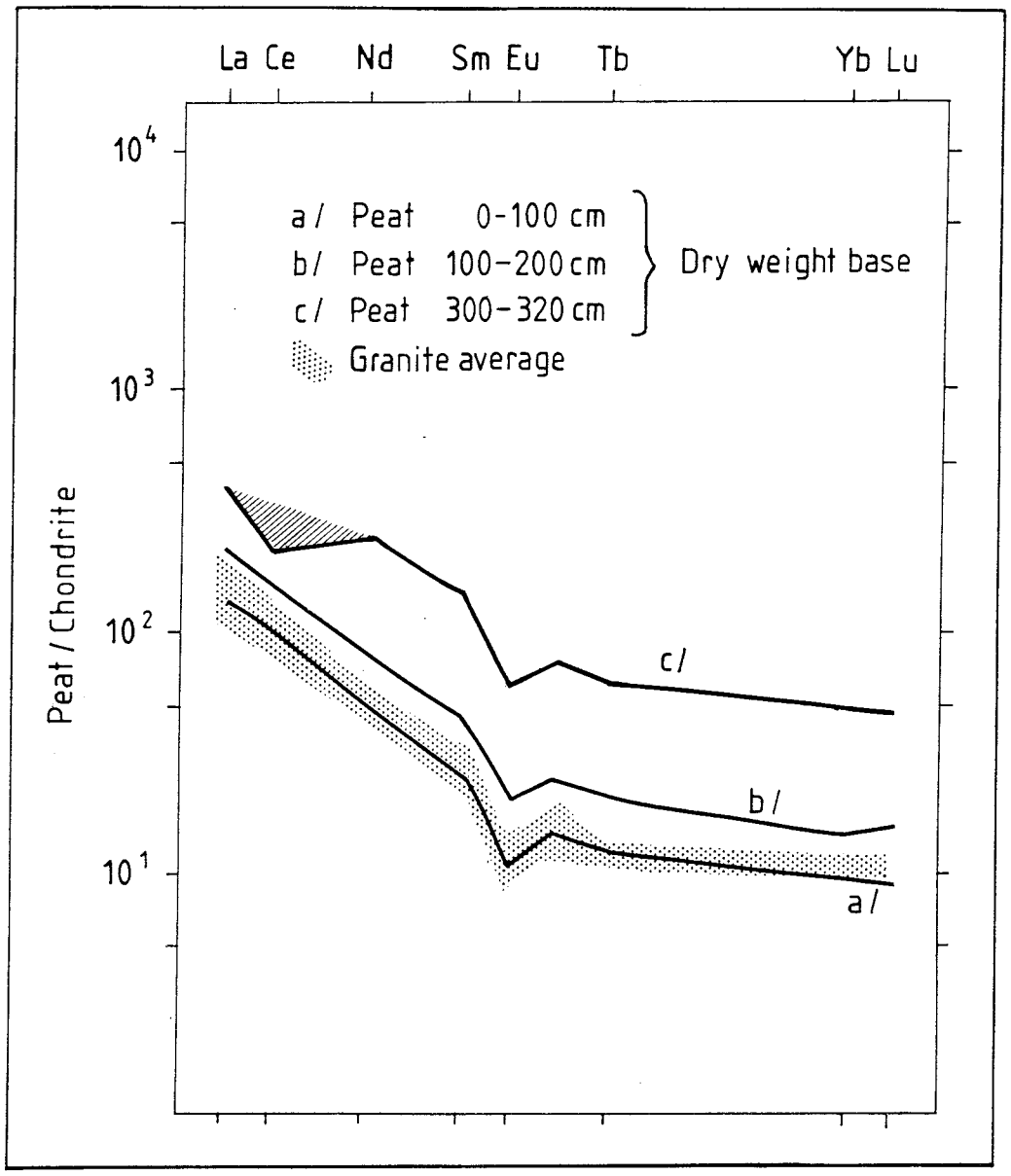

Figure 28. Chondrite-normalised REE patterns of peat and granite from the Klipperås study site.

REEs in the peat have been supplied as solutes (rather than as particulates) in ground- and surface water (Landström & Sunblad, in prep.). If no fractionation of the REEs occurs when the REEs are sorbed on the peat, the REE pattern of the peat will reflect that of the water flowing into the bog (cf. section 5.5).

The observed strong selective uptake of the light REEs on most fracture coatings is of special interest as light REEs are preferred as chemical analogues of Pu (the best analogue is Nd, according to Chapman et al., 1984). An understanding of the processes that fractionate the light REEs should thus provide a better and, moreover, a site-specific basis for predictions of the migration of Pu (as well as Am and Cm).

The mineral phases which probably constitute the main "traps" for the light REEs are Fe-oxyhydroxide and to some extent, hematite. This is in agreement with the high K_d values of the light REEs for the hydraulically most conductive Fe-oxyhydroxide/ hematite-coated fractures shown in Table 8. In contrast, the heavy REEs seem to be selectively sorbed or coprecipitated on the carbonate phases (Table 6 and fig 30). This was also observed, for fracture filling calcites, in the Bohus granite at Fjällbacka (Eliasson et al., 1990).

Sr and Cs

Ion exchange is considered to be the main sorption process for both Sr and Cs in laboratory studies, and higher K_d's were obtained for Cs in all rocks and minerals studied; the only mineral where Sr showed higher K_d's than Cs was bentonite (Andersson, 1983). In this study as well, the in situ K_d's for Cs were higher than those for Sr.

The "in situ" K_d values for Cs vary considerably (Table 8), but seem to be higher for samples containing illite, mixed-layer clay or smectite. This is not surprising as K is present in these mineral phases and Cs is known to replace K by ion exchange (cf. results presented by e.g. Ticknor et al., 1989). Similarly, sorption of Sr is favoured by Ca, and to some extent Na minerals.

Comparison between "in situ" and laboratory-determined K_d's.

Laboratory-based K_d values, as presented in the litterature, exhibit large variations depending on e.g. the solid phase, the reaction time, etc. In a first attempt to compare "in situ" and laboratory-based K_d's (Fig.29) ranges of the different K_d's are therefore used. Values of laboratory K_d's were taken from Andersson (1983) and Kipatsi (1983). Andersson (1983) gives the variation 0-0.1 m^3/kg for Sr, 0.1-1.0 m^3/kg for Cs and 1.0-10 m^3/kg for the actinides (U, Np, Pu, Am, and Th). Higher values have been obtained for special minerals e.g. 2.9 and 1.4 m^3/kg for Sr and Cs, respectively, in bentonite (Andersson 1983). These extreme values are not represented in the figure. Laboratory K_d's for Eu were taken from Wolfsberg et al. (1979) (tuff) and Eriksson & Locklund (1989) (granite).

The "in situ" K_d's used are the ranges obtained for fracture filling/groundwater pairs (Hf-corrected) in this study (Table 8). In this case as well, some extreme values are omitted (such as the extremely high Cs value recorded for Kl 2:329.65 m).

There is an obvious correlation between the two sets of data, although the laboratory K_d's are one to two orders of magnitude lower. When comparing the two K_d's one must, however, be aware of the quite different basis on which they have been determined.

Laboratory-based K_d's have been measured in batch and/or column experiments on mostly whole rock samples of various compositions but also on mineral separates and fracture fillings. Especially whole rock samples may have mineral compositions which differ strongly from those in fracture fillings. Low sorption capacity minerals, e.g. quartz and feldspar, are dominant constituents of granitic rocks, whereas the fracture fillings have higher proportions of minerals that participate more actively in the sorption processes (e.g. hematite/Fe-oxyhydroxide, carbonates, clay minerals and phyllo-silicates such as chlorite). This is also exemplified in sorption studies carried out on primary and secondary minerals from the gabbroic pluton in East Bull Lake, Canada (Ticknor et al., 1989). Secondary minerals such as kaolinite, laumontite, hornblende and biotite showed higher sorption capacities for the elements Sr, Cs, Ce and Am than the primary rock-forming minerals plagiocalse and pyroxene.

The reaction times are extremely different with a maximum of

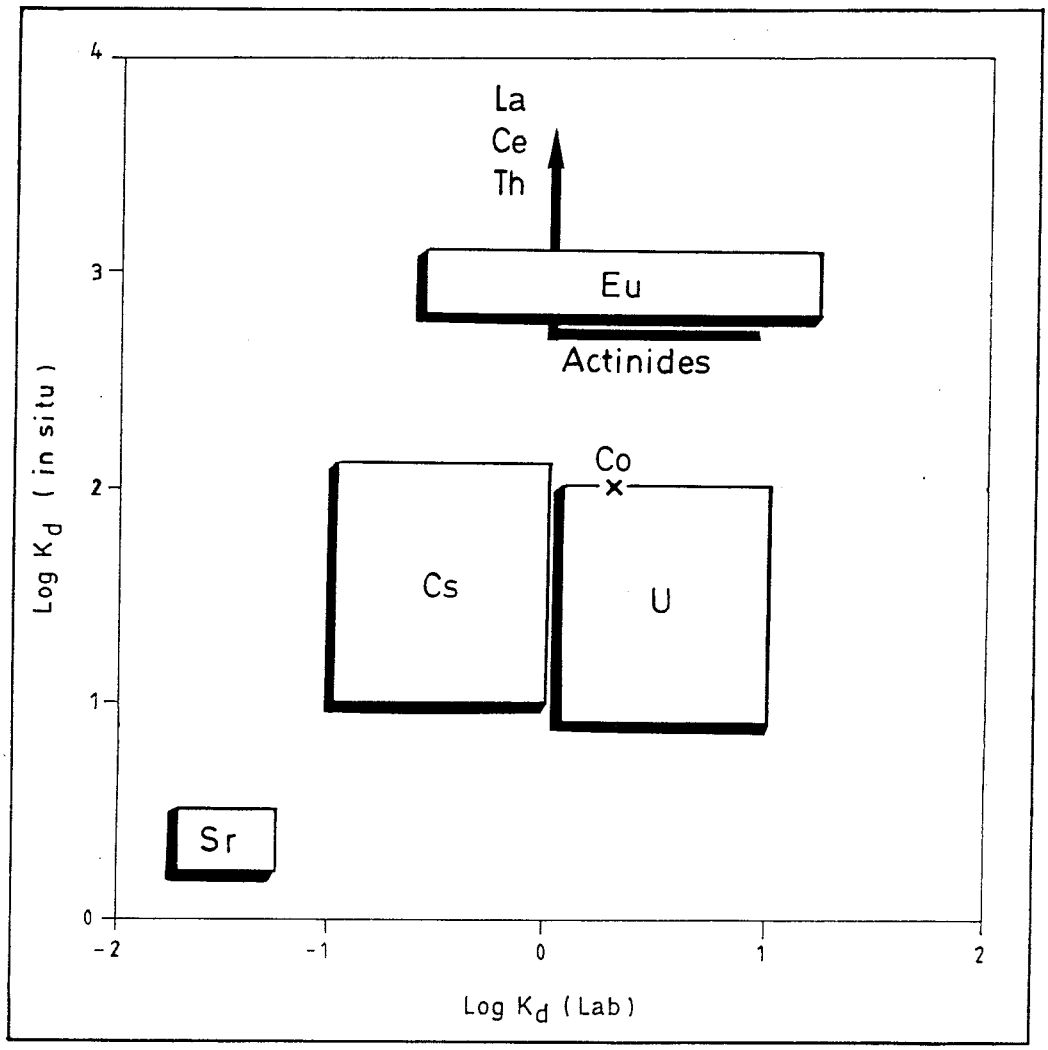

Figure 29. Laboratory-based K_d-values (Andersson; 1983 and Eriksson & Locklund; 1989) plotted versus "in situ" K_d-values (results from present study). The values are given in m^3/kg.

about one year in laboratory experiments and varying from thousands to millions of years for "in situ" K_d's. This is probably another important reason for the difference in size between the two sets of values. One explanation for the small difference between the K_d values (laboratory and "in situ") for uranium could be that uranium equilibrates with the groundwater more rapidly (compared to e.g. the REEs). Redox conditions, presence of different complexing agents, etc, are known to cause large variations in uranium mobility.

Especially the "whole sample", but also to some extent the Hf-corrected "in situ" K_d's may include minerals not very active in present mineral/groundwater interaction. As has been done in the studies by Ivanovich et al. (1988) and Dearlove et al. (1989), selective measurements of K_d's for fracture mineral separates should be performed. Low-temperature fracture coatings such as clay minerals, carbonates and Fe-oxyhydroxide are then the most important groups of minerals to be investigated as they 1) are common minerals in water conducting fractures and can form and remain stable at low temperatures, and 2) probably have sorption capacities distinctly different from that of the host rock (e.g. granite).

Investigations carried out in the granitic Eye-Dashwa pluton in Canada (Kamineni, 1986) showed that common sinks for U and REEs are epidote, sphene, calcite and gypsum. Of these minerals sphene has not been found to be a common mineral in fractures in the areas investigated by SKB. Gypsum, a low temperature mineral, has only been identified in the Sternö area and in minor amounts at Äspö. No trace element analyses of these gypsum coatings have been carried out. Epidote is a hydrothermal mineral and thus does not form under the conditions prevailingin the bedrock and, is frequently observed in zones which are water-conducting, which means its sorption capacity is important to estimate.

Following is a brief description of the trace element distributions in the three mineral groups: carbonate minerals, Fe-oxyhydroxide/hematite and clay minerals (including chlorite).

Carbonate minerals

Carbonates (mostly calcite) are common minerals in water conducting fractures, and the interaction between trace elements in water and calcite is therefore of interest. Stable isotope studies have shown that calcite precipitation/dissolution is an ongoing process in the groundwater environment encountered in the Swedish bedrock (Tullborg, 1989). Trace elements can be incorporated in the calcite lattice during precipitation or sorbed on the calcite surfaces. This means that it is necessary to find out where calcite is dissolved or precipitated to be able to estimate the order of retention of e.g. radionuclides.

Elements such as Mg, Mn and Fe are usually found in minor amounts in fresh water carbonates. Sr also fits well in the calcite lattice and it is assumed that the concentration of Sr in calcite is strongly correlated to the Sr concentration in the water responsible for the calcite formation.

Studies of adsorption and coprecipitation of Nd on calcite have been carried out by Bruno et al. (1989). They show that Nd is removed from groundwater and concentrated on carbonate surfaces. At low concentrations of Nd in the water, sorption seems to be the main process, whereas at higher concentrations coprecipitation is suggested.

Analyses of REEs in calcites from Klipperås, Lansjärv (Landström et al., 1989) and Fjällbacka (Eliasson et al., 1989) show that the concentrations of heavy REEs are relatively high in calcites as compared to other fracture minerals (and also compared to the host granite itself) (Fig. 30). Heavy REEs tend to form stronger carbonate complexes, which is reflected in their tendency to be incorporated or sorbed on calcite (Möller et al.,1979). For a single hydrothermal event, a decreasing La/Yb ratio for carbonate minerals towards the end of the event is observed, i.e. decreasing temperature (which means increased carbonate content) results in carbonates enriched in heavy REEs. This is also observed in Fjällbacka (Eliasson et al., 1989), where five calcites from one and the same hydrothermal period show a correlation between La/Yb ratio and $\delta^{18}O$ values indicative of the same processes as described by Möller et al. (1979).

The amounts of REEs in fracture carbonates seem to be correlated to the REE contents of the host rocks (Fig. 30).

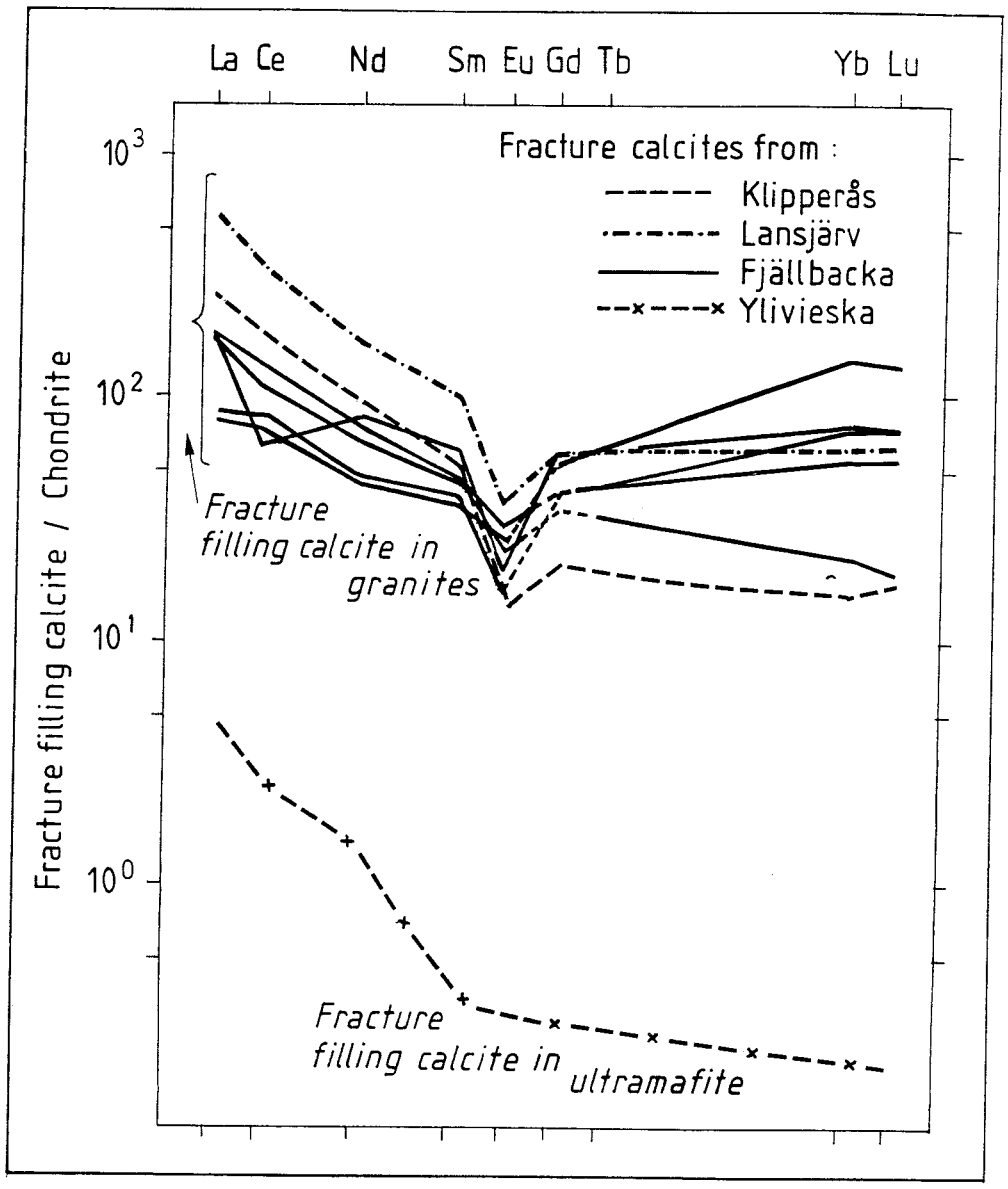

Figure 30. Chondrite-normalised REE patterns for fracture calcites from granites in Klipperås, Fjällbacka, Lansjärv and from ultramafite in Ylivieska, Finland.

Compared to granitic host rock (Klipperås and Fjällbacka) an ultramafite in Ylivieska, Finland has much lower REE contents in fracture calcites (Fig. 30). Ultramafic rocks usually show REE contents about one to two orders of magnitude lower than granitoids.

Strong enrichment of REEs in calcite can occur. For example, calcite fillings in the Eye-Dashwa pluton (Canada) showed REE concentrations c. 30 times higher than the host granite (Kamineni, 1986).

The uranium and thorium concentrations are generally low in the calcite samples analysed (especially the pure samples) and usually much lower than in the hematite/Fe-oxyhydroxide fracture coatings. The U/Th ratio is mostly >1 in the calcites, reflecting the higher mobility of uranium, compared to thorium, in the groundwater.

Fe-oxyhydroxide and hematite

Hematised zones are often water-conducting (as can be seen in Klipperås and at Äspö (Tullborg, 1988)) and the most conductive parts of the zones are usually characterized by the presence of Fe-oxyhydroxides which have high sorption capacities. As shown in this study and in laboratory experiments Fe-oxyhydroxides easily sorb uranium, thorium and REEs, especially light REEs. It is also suggested that uranium is precipitated onto Fe-oxyhydroxide phases in the near-surface transition zone, where oxidising conditions turn into reducing conditions.

In order to understand the potential for radionuclide sorption on Fe-oxyhydroxide it is necessary to understand the processes responsible for the formation of Fe-oxyhydroxide in groundwater environments in crystalline rocks. Fe-oxyhydroxide may have been formed as a last phase of an oxidising hydrothermal event (often connected with the production of hematite) and/or it may be formed by ongoing interaction between present groundwater (reducing) and existing Fe(III) minerals such as hematite. If it can be shown that Fe-oxyhydroxide forms from present groundwater under low-temperature conditions, this means that all the trace elements found in the Fe-oxyhydroxide are mobilised/sorbed under conditions similar those at present. Otherwise, at least a portion of the trace element content in the Fe-oxyhydroxide probably originates

from hydrothermal solutions. It is proposed that trace element analyses of separated phases of Fe-oxyhydroxide and hematite should be made. Furthermore, $\delta^{18}O$ and δD analyses of Fe-oxyhydroxide and hematite are proposed in order to permit determination of the origin of Fe-oxyhydroxide from different depths (cf. Yapp, 1987).

Manganese is often associated with Fe-oxyhydroxide, and it seems as if the presence of Mn in oxyhydroxide phases can further increase the sorption or coprecipitation of REEs, especially Ce^{4+} (cf. manganese nodules on the ocean floor). Unfortunately, it has not been possible to carry out any Mn analyses within this project.

Clay minerals and chlorite

The clay minerals analysed for trace element composition in this study are illite, mixed-layer clay and smectite (the latter in in situ migration experiments in Studsvik, Landström et al., 1983). These are the most frequent clay minerals in fractures in crystalline rocks at great depth. However, the amounts of clay minerals in the water-conducting fractures in Klipperås are generally low (except for single fracture zones) compared to the frequency of hematite/Fe-oxyhydroxide, chlorite and calcite.

The clay minerals analysed mostly showed trace element distributions that agreed closely with that of the host rock, although an enrichment of certain elements can be observed, especially in water-conducting clay-coated fractures. For instance, cesium shows very selective sorption on clay minerals. It is also known that the dominant sorption process responsible for the Cs upptake is ion exchange, and that this is at least partly irreversible (Andersson, 1983).

Uranium can also be selectively sorbed on clay minerals which is exemplified in sample Kl 10:21.7 m in Klipperås (cf. also Dearlove et al., 1989; and Ivanovich et al.,1988). Although not observed in the samples from Klipperås sorption of thorium on clay minerals is evident from the investigations of Dearlove et al.(1989) and Ivanovich et al. (1988).

The clay minerals analysed from Klipperås show REE patterns similar to that of the host granite and there is no evidence of

fractionation of these elements. This was also observed in the Lansjärv study (Landström et al., 1989)

Chlorite is a mineral frequently observed in water-conductive fractures within the Swedish bedrock. Its sorption capacity is thus important when estimating radionuclide migration along fractures. Chlorite might also form at slightly elevated temperatures (c. 100°C (Kam et al., 1984) i.e. close to temperatures assumed to prevail in the near-field of a radwaste disposal). This means that it can act as a sink, by incorporation of radionuclides in the lattice, in the vicinity of a radwaste disposal. In the fracture fillings analysed from Klipperås and Lansjärv (Landström et al., 1989) chlorite is present in several samples. However, it has not been possible from the trace element distribution patterns to distinguish any specific sorption capacity of the chlorite and analyses of mineral separates are needed.

6. CONCLUSION

The element contents of fracture fillings vary widely compared to the host rocks. U varies in analysed granite samples between 3.5-10.6 ppm and in fracture fillings between 9-400 ppm. The corresponding Th values are 16-27 ppm and 2.6-307 ppm, respectively, and for La 36-70 ppm and 22-4500 ppm, respectively. These figures also reflect the wide range in sorption capacities of different fracture mineral groups. It is thus necessary to gain good knowledge of the distribution of trace elements and indirectly of sorption capacities in fracture fillings within potential site environments.

The different chemical analogues have shown marked selectivities for certain fracture mineral groups and studies of separated phases are recommended to obtain a better understanding of these effects. Some main findings for the different elements are described in brief below:

U is sorbed on most of the studied material and seems to be selectively sorbed on Fe phases. From the in situ K_d measurements one can conclude that U is more mobile (relative to the other elements) than expected from laboratory sorption experiments. The reason for this has not yet been determined.

Th has been mobilised, and for this element as well the Fe phases seem to constitute the main sinks. No mobilisation of Th was observed in connection with clay alteration processes.

REE: Since individual REEs possess varying qualifications as chemical analogues for the actinides, the sometimes extreme fractionation of the REEs in certain fracture fillings is of great interest. Determining which mineral phases are responsible for this and during which time periods the sorption has occured are important tasks for future studies. A selectivity for Fe phases was found for the light REEs, whereas the carbonate phases show a selective sorption of the heavy REEs. The sorption of REEs on clay minerals seems to be insignificant, and no fractionation tendencies were observed in these phases.

Cs is mobile and seems to be selectively sorbed on the clay mineral phases.

In situ K_d's determined here are based on the net element concentration added to the fracture filling sample from the fluid phase as the result of a complex of processes taking place over a

very long period of time. It is probable that only parts of the fracture fillings have reacted with the present groundwater and this, together with the time effect, are the main reasons for the higher in situ K_d's (on average a factor of 100 higher for Sr, Cs, Co, Eu and about 10 for U) compared to the laboratory-based ones.

The correlation between in situ and laboratory K_d's indicates that the relative mobilities of studied radionuclides as predicted from laboratory experimental data will be valid in a fractured granitic environment over a long time perspective. The in situ K_d's suggest, however, a higher mobility for U, relative to the other elements, than is expected from the laboratory K_d's.

ACKNOWLEDGEMENT

This report is the result of collaboration and interaction between a number of researchers and colleagues to whom we are very grateful.

Andrzej Olkiewicz has provided rock and fracture samples, offered comments on geological aspects and helped us with the literature search at the Royal Institute of Technology in Stockholm.

Peter Wikberg provided the groundwater samples.

Jordi Bruno and Ingemar Grenthe (Royal Institute of Technology), Fred Karlsson and Peter Wikberg (SKB, Stockholm), Otto Brotzen and John Smellie have made valuable comments during the work and proposed improvements to the manuscript.

Kristina Kling drew the figures with great skill.

REFERENCES

Aftalion, M., Fallick, A.E. and Wilson, M.R. (1981) Age and isotope studies in Norrbotten and Småland: Preliminary results. Geol. Fören. Stockholm. Förh. vol 103, pp 519-520.

Andersson, K. (1984) Transport of radionuclides in water/mineral systems. Ph D thesis. Chalmer University of Technology , Göteborg. ISBN 91-7032-105-1.

Almèn, K.E., Andersson, O., Fridh, B., Johansson, B-E., Sehlstedt, S., Hansson, K., Olsson, O., Nilsson, G. and Wikberg, P. (1986) Site investigations - equipment for geological, geophysical, hydrogeological and hydrochemical characterization. SKB Technical Report TR 86-16.

Bruno, J., Carrol, S., Sandino, A., Charlet, L., Karthein, R. and Wersin, P. (1989) Adsorption, precipitation and coprecipitation of trace metals on carbonate minerals at low temperatures. Extended abstract Water-Rock Interaction, Miles (ed) pp 121-124. Balkema, Rotterdam, ISBN 90 6191 9703.

Chapman, N.A., McKinley, I.G. and Smellie, J.A.T. (1984). The potential of natural analogues in assessing systems for deep disposal of high-level radioactive waste. In: Natural analogues to the conditions around a final respository for high-level radioactive waste. Proceedings of the natural analogue workshop held at Lake Geneva, Wisconsin, U.S.A. (october 1-3, 1984). SKB Technical Report, TR 84-18.

Dearlove, J.P.I., Ivanovich, M. and Green, D.C. (1989) Partition coefficients (R_d) for the U series radionuclides in ion exchange sites and amorphous Fe phase in illite and granite samples. Extended abstract Water-Rock Interaction, Miles (ed) pp 191-194. Balkema, Rotterdam, ISBN 90 6191 9703.

Drake, M.J. and Weill, D.F. (1975) Partion of Sr, Ba, Ca, Y, Eu^{3+}, Eu^{4+} and other REE between plagioclase feldspar and magmatic liquid: an experimental study. Geochim. Cosmochim. vol 39, pp 669-712.

Eliasson, T., Tullborg, E-L. and Landström, O. (1990) Fracture filling mineralogy and geochemistry at the Swedish HDR research site. In Int. Hot Dry Rock Geothermal Energy Conf. Proceed. Pergamon, Oxford. (In press).

Eriksen, T.E. and Locklund, B. (1989) Radionuclide sorption on crushed and intact granitic rock - Volume and surface effects. SKB Technical Report TR 89-25.

Ferri, D., Grenthe, I., Hietanen, S. and Salvatore, F. (1983) Studies on metal carbonate complexes in aqueous perchlorate media. Acta Chemica Scandinavica A 37, pp 359-365.

Fritz, B., Kam, M. and Tardy, Y (1984). Geochemical simulation of the evolution of granitic rocks and clay minerals submitted to a temperature increase in the vicinity of a respository for spent nuclear fuel.

Gentzschein, B. (1986) Hydrogeological investigations at the Klipperås study site. SKB technical Report TR-86-08.

Henderson, P. (ed) (1984) Rare earth element geochemistry. Elsevier, Amsterdam, ISBN 0-444-42148-3

Holst, N.O. (1879) Geological description of map sheet Lessebo. (In Swedish) Swedish Geological Survey (SGU). Ab 4.

Holst, N.O. (1893) Geological description of map sheet Lenhofda. (In Swedish) Swedish Geological Survey (SGU). Ab 15.

Ivanovich, M., Longworth, G., Wilkins, M.A., Hasler, S.E. and Lloyd, M.J. (1988) Measurement of effective K_d factors for the long-lived uranium and thorium isotopes in samples of London Clay (Bradwell) and mudrock (Fullbeck). Nirex Report NSS-R117.

Kamineni, D. C. (1986) Distribution of Uranium, Thorium and rare-earth elements in the Eye-Dashwa lakes pluton - A study of some analogue elements. Chem. Geol. vol 55, pp 361-373.

Kipatsi, H. (1983) Sorption behaviour of long-lived fission products and actinides in clay and rock. Ph D Thesis. Department of nuclear chemistry, Chalmers University of Technology, Göteborg, Sweden. ISBN 91-7032-085-3.

Landström, O., Klockars, C-E, Persson, O., Tullborg, E-L., Larson, S.Å., Andersson, K. and Allard, B. (1983) Migration experiments in Studsvik. SKBF/KBS, Technical Report TR 83-18

Landström, O. and Sundblad, B. (1986) Migration of thorium, uranium, radium and Cs-137 in till and soils and their uptake in organic matter and peat. SKB Technical Report TR 86-24.

Landström, O., Smellie, J. and Tullborg, E-L. (1989) Mineralogical and geochemical studies of fracture infillings in drillcore KLJ 1. In: Interdisiplinary-study of post-glacial faulting in the Lansjärv area, northern Sweden 1986-1988, SKB TR 89-31.

Laurent, S. (1986) Analyses of groundwater from deep boreholes in Klipperås. SKB Technical Reort TR 86-17.

Middelburg, J.J., Van der Weijden, C.H. and Woittiez, J.R.W. (1988) Chemical processes affecting the mobility of major, minor and trace elements during weathering of granitic rocks. Chem. Geol. vol 68, pp 253-273.

Möller P., Morteani, G., Hoefs, J. and Parekh, P.B. (1979). The origin of the ore bearing solution in the Pb-Zn veins of the western Harz/Germany as deduced from rare element and isotope distribution in calcite. Chem. Geol., vol 26, pp 197-225.

Magnusson, N.H. (1960) Age determinations of Swedish Precambrian rocks. Geol. Föten. Stockholm Förh. vol 59, pp 205-228.

Nesbitt, H.W. (1979) Mobility and fractionation of REE during weathering of a granodiorite. Nature, vol 279, pp 206-210.

Olkiewicz, A. and Stejskal, V. (1986) Geological and tectonical description of the Klipperås study site. SKB Technical Report TR 86-06.

Patchett, P.J. (1978) Rb/Sr ages of Precambrian dolerites and syenites in southern and central Sweden. Swedish Geological survey Ser. C 747, pp 1-63.

Sehlstedt, S. and Stenberg, L. (1986) Geophysical investigations at the Klipperås study site. SKB Technical Report TR 86-17.

Smellie, J., Larsson, N.Å., Wikberg, P., Puigdoménech, I. and Tullborg, E-L. (1987) Hydrochemical investigations in crystalline bedrock in relation to existing hydraulic conditions: Klipperås test-site, Småland, Southern Sweden. SKB Technical Report TR 87-21.

Ticknor, K.V., Vandergraaf, T.T. and Kamineni, D.C. (1989) Radionuclide sorption on primary and fracture-filling minerals from East Bull Lake pluton, Massey, Ontario, Canada. Applied Geochemistry, vol 4, pp 163-176.

Tullborg, E-L. (1986) Fissure fillings from the Klipperås study site. SKB Technical Report TR 86-10.

Tullborg, E-L (1988) Fracture fillings in the drill cores from Äspö and Laxemar. SKB/PR 25-88-11.

Tullborg, E-L. (1989) $\delta^{18}O$ and $\delta^{13}C$ in fracture calcite used for interpretation of recent meteoric water circulation. Extended abstract, Water-Rock interaction, Miles (ed), pp 695-698, Balkema, Rotterdam, ISBN 90 6191 9703.

Tullborg, E-L. (1989) The influence of recharge water on fissure filling minerals - A study from Klipperås, southern Sweden. Chem. Geol. vol 76, pp 309-320.

Yapp, C.J. (1987) Oxygen and hydrogen isotope variation among goethites (α-FeOOH) and the determination of paleotemperatures.Geochim. Cosmochim. Acta, vol 51, pp 355-364.

Wolfsberg, K., Bayhurst, B.P., Crowe, B.M., Daniels, W.R., Erdal, B.R., Lawrence, F.O., Norris, A.E. and Smyth, J.R. (1979) Sorption-desorption studies on tuff. 1. initial Studies with samples from J-13 drill site, Jackass Flats, Nevada. LA-7480-MS, Informal Report, UC-11 and UC 70.

Åberg, G. (1978) Precambrian geochronology of south-eastern Sweden. Geol. Fören. Stockholm Förh. vol 100, pp 125-154.

List of SKB reports

Annual Reports

1977–78
TR 121
KBS Technical Reports 1 – 120.
Summaries. Stockholm, May 1979.

1979
TR 79–28
The KBS Annual Report 1979.
KBS Technical Reports 79-01 – 79-27.
Summaries. Stockholm, March 1980.

1980
TR 80–26
The KBS Annual Report 1980.
KBS Technical Reports 80-01 – 80-25.
Summaries. Stockholm, March 1981.

1981
TR 81–17
The KBS Annual Report 1981.
KBS Technical Reports 81-01 – 81-16.
Summaries. Stockholm, April 1982.

1982
TR 82–28
The KBS Annual Report 1982.
KBS Technical Reports 82-01 – 82-27.
Summaries. Stockholm, July 1983.

1983
TR 83–77
The KBS Annual Report 1983.
KBS Technical Reports 83-01 – 83-76
Summaries. Stockholm, June 1984.

1984
TR 85–01
Annual Research and Development Report 1984
Including Summaries of Technical Reports Issued during 1984. (Technical Reports 84-01– 84-19)
Stockholm June 1985.

1985
TR 85-20
Annual Research and Development Report 1985
Including Summaries of Technical Reports Issued during 1985. (Technical Reports 85-01-85-19)
Stockholm May 1986.

1986
TR 86-31
SKB Annual Report 1986
Including Summaries of Technical Reports Issued during 1986
Stockholm, May 1987

1987
TR 87-33
SKB Annual Report 1987
Including Summaries of Technical Reports Issued during 1987
Stockholm, May 1988

1988
TR 88-32
SKB Annual Report 1988
Including Summaries of Technical Reports Issued during 1988
Stockholm, May 1989

Technical Reports

List of SKB Technical Reports 1990

TR 90-01
FARF31 –
A far field radionuclide migration code for use with the PROPER package
Sven Norman[1], Nils Kjellbert[2]
[1] Starprog AB
[2] SKB AB
January 1990

TR 90-02
Source terms, isolation and radiological consequences of carbon-14 waste in the Swedish SFR repository
Rolf Hesböl, Ignasi Puigdomenech, Sverker Evans
Studsvik Nuclear
January 1990

TR 90-03
Uncertainties in repository performance from spatial variability of hydraulic conductivities –
Statistical estimation and stochastic simulation using PROPER
Lars Lovius[1], Sven Norman[1], Nils Kjellbert[2]
[1] Starprog AB
[2] SKB AB
February 1990

TR 90-04
Examination of the surface deposit on an irradiated PWR fuel specimen subjected to corrosion in deionized water
R.S. Forsyth, U-B. Eklund, O. Mattsson, D. Schrire
Studsvik Nuclear
March 1990

TR 90-05
Potential effects of bacteria on radionuclide transport from a Swedish high level nuclear waste repository
Karsten Pedersen
University of Gothenburg, Department of General and Marine Microbiology, Gothenburg
January 1990

TR 90-06
Transport of actinides and Tc through a bentonite backfill containing small quantities of iron, copper or minerals in inert atmosphere
Yngve Albinsson, Birgit Sätmark, Ingemar Engkvist, W. Johansson
Department of Nuclear Chemistry, Chalmers University of Technology, Gothenburg
April 1990

TR 90-07
Examination of reaction products on the surface of UO_2 fuel exposed to reactor coolant water during power operation
R S Forsyth, T J Jonsson, O Mattsson
Studsvik Nuclear
March 1990

TR 90-08
Radiolytically induced oxidative dissolution of spent nuclear fuel
Lars Werme[1], Patrik Sellin[1], Roy Forsyth[2]
[1] Swedish Nuclear Fuel and waste Management Co (SKB)
[2] Studsvik Nuclear
May 1990

TR 90-09
Individual radiation doses from unit releases of long lived radionuclides
Ulla Bergström, Sture Nordlinder
Studsvik Nuclear
April 1990

TR 90-10
Outline of regional geology, mineralogy and geochemistry, Poços de Caldas, Minas Gerais, Brazil
H D Schorscher[1], M E Shea[2]
[1] University of Sao Paulo
[2] Battelle, Chicago
December 1990

TR 90-11
Mineralogy, petrology and geochemistry of the Poços de Caldas analogue study sites, Minas Gerais, Brazil. I: Osamu Utsumi uranium mine
N Waber[1], H D Schorscher[2], A B MacKenzie[3], T Peters[1]
[1] University of Bern
[2] University of Sao Paulo
[3] Scottish Universities Research & Reactor Centre (SURRC), Glasgow
December 1990

TR 90-12
Mineralogy, petrology and geochemistry of the Poços de Caldas analogue study sites, Minas Gerais, Brazil. II: Morro do Ferro
N Waber
University of Bern
December 1990

TR 90-13
Isotopic geochemical characterisation of selected nepheline syenites and phonolites from the Poços de Caldas alkaline complex, Minas Gerais, Brazil
M E Shea
Battelle, Chicago
December 1990

TR 90-14
Geomorphological and hydrogeological features of the Poços de Caldas caldera, and the Osamu Utsumi mine and Morro do Ferro analogue study sites, Brazil
D C Holmes[1], A E Pitty[2], R Noy[1]
[1] British Geological Survey, Keyworth
[2] INTERRA/ECL, Leicestershire, UK
December 1990

TR 90-15
Chemical and isotopic composition of groundwaters and their seasonal variability at the Osamu Utsumi and Morro do Ferro analogue study sites, Poços de Caldas, Brazil
D K Nordstrom[1], J A T Smellie[2], M Wolf[3]
[1] US Geological Survey, Menlo Park
[2] Conterra AB, Uppsala
[3] Gesellschaft für Strahlen- und Umweltforschung (GSF), Munich
December 1990

TR 90-16

Natural radionuclide and stable element studies of rock samples from the Osamu Utsumi mine and Morro do Ferro analogue study sites, Poços de Caldas, Brazil

A B MacKenzie[1], P Linsalata[2], N Miekeley[3], J K Osmond[4], D B Curtis[5]
[1] Scottis Universities Research & Reactor Centre (SURRC), Glasgow
[2] New York Medical Centre
[3] Catholic University of Rio de Janeiro (PUC)
[4] Florida State University
[5] Los Alamos National Laboratory
December 1990

TR 90-17

Natural series nuclide and rare earth element geochemistry of waters from the Osamu Utsumi mine and Morro do Ferro analogue study sites, Poços de Caldas, Brazil

N Miekeley[1], O Coutinho de Jesus[1], C-L Porto da Silveira[1], P Linsalata[2], J N Andrews[3], J K Osmond[4]
[1] Catholic University of Rio de Janeiro (PUC)
[2] New York Medical Centre
[3] University of Bath
[4] Florida State University
December 1990

TR 90-18

Chemical and physical characterisation of suspended particles and colloids in waters from the Osamu Utsumi mine and Morro do Ferro analogue study sites, Poços de Caldas, Brazil

N Miekeley[1], O Coutinho de Jesus[1], C-L Porto da Silveira[1], C Degueldre[2]
[1] Catholic University of Rio de Janeiro (PUC)
[2] PSI, Villingen, Switzerland
December 1990

TR 90-19

Microbiological analysis at the Osamu Utsumi mine and Morro do Ferro analogue study sites, Poços de Caldas, Brazil

J West[1], A Vialta[2], I G McKinley[3]
[1] British Geological Survey, Keyworth
[2] Uranio do Brasil, Poços de Caldas
[3] NAGRA, Baden, Sitzerland
December 1990

TR 90-20

Testing of geochemical models in the Poços de Caldas analogue study

J Bruno[1], J E Cross[2], J Eikenberg[3], I G McKinley[4], D Read[5], A Sandino[1], P Sellin[6]
[1] Royal Institute of Technology (KTH), Stockholm
[2] AERE, Harwell, UK
[3] PSI, Villingen, Switzerland
[4] NAGRA, Baden, Switzerland
[5] Atkins ES, Epsom, UK
[6] Swedish Nuclear and Waste Management Co (SKB), Stockholm
December 1990

TR 90-21

Testing models of redox front migration and geochemistry at the Osamu Utsumi mine and Morro do Ferro analogue sites, Poços de Caldas, Brazil

J Cross[1], A Haworth[1], P C Lichtner[2], A B MacKenzi[3], L Moreno[4], I Neretnieks[4], D K Nordstrom[5], D Read[6], L Romero[4], S M Sharland[1], C J Tweed[1]
[1] AERE, Harwell, UK
[2] University of Bern
[3] Scottish Universities Research & Reactor Centre (SURRC), Glasgow
[4] Royal Institute of Technology (KTH), Stockholm
[5] US Geological Survey, Menlo Park
[6] Atkins ES, Epsom, UK
December 1990

TR 90-22

Near-field high temperature transport: Evidence from the genesis of the Osamu Utsumi uranium mine analogue site, Poços de Caldas, Brazil

L M Cathles[1], M E Shea[2]
[1] University of Cornell, New York
[2] Battelle, Chicago
December 1990

TR 90-23

Geochemical modelling of water-rock interactions at the Osamu Utsumi mine and Morro do Ferro analogue sites, Poços de Caldas, Brazil

D K Nordstrom[1], I Puigdomenech[2], R H McNutt[3]
[1] US Geological Survey, Menlo Park
[2] Studsvik Nuclear, Sweden
[3] McMaster University, Ontario, Canada
December 1990

TR 90-24
The Poços de Caldas Project: Summary and implications for radioactive waste management
N A Chapman[1], I G McKinley[2], M E Shea[3], J A T Smellie[4]
[1] INTERRA/ECL, Leicestershire, UK
[2] NAGRA, Baden, Switzerland
[3] Battelle, Chicago
[4] Conterra AB, Uppsala

TR 90-25
Kinetics of UO_2(s) dissolution reducing conditions: numerical modelling
I Puigdomenech[1], I Cass[2], J Bruno[3]
[1] Studsvik AB, Nyköping, Sweden
[2] Department of Chemical Engineering, E.T.S.E.I.B. (U.P.C.), Barcelona, Spain
[3] Department of Inorganic Chemistry, The Royal Institute of Technology, Stockholm, Sweden
May 1990

TR 90-26
The effect from the number of cells, pH and lanthanide concentration on the sorption of promethium on gramnegative bacterium (Shewanella Putrefaciens)
Karsten Pedersen[1], Yngve Albinsson[2]
[1] University of Göteborg, Department of General and Marine Microbiology, Gothenburg, Sweden
[2] Chalmers University of Technology, Department of Nuclear Chemistry, Gothenburg, Sweden
June 1990

TR 90-27
Isolation and characterization of humics from natural waters
B Allard[1], I Arsenie[1], H Borén[1], J Ephraim[1], G Gårdhammar[2], C Pettersson[1]
[1] Department of Water and Environmental Studies, Linköping University, Linköping, Sweden
[2] Department of Chemistry, Linköping University, Linköping, Sweden
May 1990

TR 90-28
Complex forming properties of natural organic acids. Part 2. Complexes with iron and calcium
James H Ephraim[1], Andrew S Mathuthu[2], Jacob A Marinsky[3]
[1] Department of Water in Environment and Society, Linköping University, Linköping, Sweden
[2] Chemistry department, University of Zimbabwe, Harare, Zimbabwe
[3] Chemistry Department, State University of New York at Buffalo, Buffalo, NY, USA
July 1990

TR 90-29
Characterization of humic substances from deep groundwaters in granitic bedrock in Sweden
C Pettersson, J Ephraim, B Allard, H Borén
Department of Water and Environmental Studies, Linköping University, Linköping, Sweden
June 1990

TR 90-30
The earthquakes of the Baltic shield
Ragnar Slunga
Swedish National Defence Research Institute
June 1990

TR 90-31
Near-field performance of the advanced cold process canister
Lars Werme
Swedish Nuclear Fuel and Waste Management Co (SKB)
September 1990

TR 90-32
Radioclide transport paths in the nearfield – a KBS-3 concept study
Roland Pusch
Clay Technology AB and Lund University of Technology
July 1990

TR 90-33
PLAN 90
Costs for management of the radioactive waste from nuclear power production
Swedish Nuclear Fuel and Waste Management Co (SKB)
June 1990

TR 90-34
GEOTAB: User's guide – Version 1.8.2
Ergodata
October 1990

TR 90-35
Dose conversion factors for major nuclides within high level waste
Ulla Bergström, Sture Nordlinder
Studsvik Nuclear
November 1990

TR 90-36
Sensitivity analysis of groundwater flow Licentiate thesis
Yung-Bing Bao
Royal Institute of Technology, Department of Land and Water Resources, Stockholm, Sweden
December 1990